AN EXPERIMENTAL INVESTIGATION OF THE NONLINEAR VIBRATION OF CYLINDRICAL SHELLS

Thesis by

Frank Kendall III

In Partial Fulfillment of the Requirements

For the Degree of

Aeronautical Engineer

California Institute of Technology

Pasadena, California

1973

(Submitted September 1973)

ACKNOWLEDGEMENTS

The author wishes to extend his sincere thanks to Dr. C. D. Babcock for his guidance during the course of this work. The assistance of Dr. E. E. Sechler during this work and throughout the author's graduate study was greatly appreciated. The author is also indebted to Dr. W. D. Iwan for his helpful suggestions. Thanks are also due to Mr. Marvin Jessey, Mr. Clarence Hemphill and Mr. Gerald Turner for their assistance with technical problems. The assistance of Mrs. Elizabeth Fox in typing the manuscript and Mrs. Betty Wood in preparing the figures and plots is acknowledged.

This work was supported by the Air Force Office of Scientific Research under Grant AFOSR 73-2447. This support is gratefully acknowledged.

Finally the author wishes to thank his wife Marjorie, without whose infinite patience and understanding this work could not have been completed.

ABSTRACT

An experimental investigation of the nonlinear vibrations of cylindrical shells was undertaken. An aluminum shell was vibrated by means of an induction shaker. An optical device was used to obtain radial displacement measurements. Several modes of vibration were studied in detail. Various nonlinear effects were observed. These included nonlinearity in the driven mode frequency response curve, the participation of the companion mode, and the participation of axisymmetric response at twice the driven frequency. The experimental results indicated only a softening type nonlinearity. The response of the companion mode was significant in several of the modes studied and was of a more complex nature than was predicted by previous theoretical work.

TABLE OF CONTENTS

LIST OF FIGURES

LIST OF FIGURES (Cont'd)

NOMENCLATURE

SYMBOL	DEFINITION
A	amplitude of driven mode response
B	amplitude of companion mode response
E	Young's Modulus
h	shell thickness
i	induction vibrator current
L	shell length
m	number of half wave in axial direction
n	number of full waves in circumferential direction
R	shell radius
u	axial displacement
v	circumferential displacement
w	radial displacement
w_m	maximum radial displacement
x	axial coordinate
y	circumferential coordinate
z	radial coordinate
α	nonlinearity parameter
γ	percentage of critical damping
δ_a	phase angle of driven mode response
δ_b	phase angle of companion mode response
ϵ	perturbation parameter, w_m/R
λ_o	$\omega_o^2 (1-\nu^2) \frac{\rho R^2}{E}$
ν	Poisson's Ratio
ρ	density

Nomenclature (Continued)

SYMBOL	DEFINITION
ω	frequency
ω_o	linear resonant frequency

I. INTRODUCTION

The study of the nonlinear vibrations of cylindrical shells has taken on some degree of importance over the past decade. Use of shell structures in aerospace applications is broad. Shell structures in such applications may be subjected to relatively high frequency loading, either aerodynamic or mechanical. This creates the need for an understanding of the dynamic behavior of structural shells subject to time dependent loading.

Analytical work in the field of nonlinear cylindrical shell vibrations has been abundant over the past twenty years. Experimental work on the other hand has been surprisingly limited. This work was undertaken in an attempt to fill the gap in experimental results and thus to provide a basis for comparison of the many existing approximate analytic solutions to the problem.

Nonlinear behavior arises in cylindrical shell vibrations on account of the relatively large contribution of the nonlinear terms in the strain displacement relations.

The most common starting point for an analysis of cylindrical shell vibrations is the well-known Donnell equations. Most of the theoretical work on the subject has begun with the study of these equations. The nonlinear terms in Donnell's equations have considerable effect on the nature of the response. Nonlinear effects are manifested primarily in three ways: (1) the nature of the response-frequency relationship in the vicinity of the linear resonant frequencies, (2) the participation of the so-called companion mode which is 90 degrees out of spatial phase with the excited mode,

and (3) the existence of an axisymmetric response at twice the driven frequency.

The linear solution indicates that there will be a standing wave vibration in conformity with the external excitation. For a point sinusoidal excitation the circumferential mode shape will be a cosine form with an antinode at the location of the point force. This mode will be referred to as the driven mode.

The nonlinearity in the driven mode response occurs in the dependence of the resonant frequency on the amplitude of the forcing function. If the resonant frequency increases with increasing forcing function amplitude the nonlinearity is of the hardening type. If the resonant frequency decreases with increasing forcing amplitude the nonlinearity is of the softening type. This is the first nonlinear effect referred to above.

The second nonlinear effect was first observed in experimental results for flutter tests at supersonic speeds (Ref. 1). These results indicated a traveling wave response. This is not predicted by linear theory. This phenomenon may, however, be explained by the inclusion of a response mode 90° out of spatial phase with the driven mode. This mode will be referred to as the companion mode. Fig. 1 shows the mode shapes of both the driven and companion modes.

The third nonlinear effect referred to is the occurrence of response at twice the driven frequency. This response is axisymmetric in nature and serves as a mechanism to relieve the membrane stresses which large amplitude driven mode vibrations create in the

shell. This response will be referred to as the axisymmetric mode.

The earliest work on the problem of nonlinear vibration is that of Reissner (Ref. 2). Subsequent work has been carried out by Chu (3), Cummings (4), Nowinski (5), Evensen (6), Dowell (7), Matsuzaki and Kobayashi (8, 9), Mayers and Wrenn (10), and Bleich and Ginsberg (11). These works are summarized by Chen (12). The main similarity of most work prior to that of Chen's is that the analysis was conducted based upon some assumption of the spatial dependence of the vibration mode. In addition, the results obtained appeared to be sensitive to details of the analysis.

Chen's (Ref. 12) work is the most recent and the most general. Of the previously mentioned works all but two (10, 11) employed a Galerkin procedure to analyze the response based on Donnell's equations. Chen investigated the response starting with Donnell's equations but used a perturbation technique. Thus his results are independent of an assumed mode shape. Chen's work will be discussed in some detail in the next section. His work will provide the basis for comparison with the experimental results.

The experimental work is, as was stated before, somewhat limited in this field. Matsuzaki and Kobayashi (9) investigated the response of a thin cylindrical shell with clamped ends. They found only softening nonlinearities in the driven mode response. Companion mode participation was observed but not studied in detail.

Olsen (13) investigated the response of an electroplated copper cylinder which was to be used in flutter experiments. His driving force was provided by an acoustical driver. Only one

mode was investigated. Softening behavior was observed for that mode. In addition his results indicated that companion modes and axisymmetric modes may have been participating in the response. No data for these modes were obtained.

Chen (12) did experimental work in conjunction with this analysis. He used the same test specimen as was employed in this work and the same driver as employed by Olsen (13). His experiment was limited primarily to the study of one mode of vibration. He found a softening nonlinearity in the driven mode response. He also observed and obtained data for the companion mode. No investigation of the axisymmetric modes was made.

The present work was undertaken to perform a complete study of several modes of vibration. A driving system was developed which would produce significantly higher amplitudes than had been attained in previous investigations. A thorough study of both axisymmetric and companion modes as well as driven modes was undertaken.

Before proceeding with a discussion of this work and its results the analytical results of Chen's work will be reviewed.

II. RESULTS OF CHEN'S ANALYSIS

Chen's analysis begins with the use of Donnell's shallow shell equations. The coordinate system and shell characteristics are shown in Fig. 2. The boundary conditions studied were the classical simply-supported conditions (SS1/SS1).

Chen employed a small perturbation method. He used maximum radial displacement over the shell radius as a small parameter ϵ and expanded the nondimensional frequency λ, radial displacement w, forcing function F, and tangential displacements u and v as power series in ϵ.

The zeroth and 1st order equations in ϵ were solved explicitly. The second order equations were not solved but the frequency response curve was obtained from the so-called secular terms whose spatial dependence corresponded to the driven mode.

The form of the solution for the radial displacement for a point sinusoidal forcing function was found to be:

$$
\begin{aligned}
w \sim\ & A \cos(\omega t + \delta_a) \cos n\frac{y}{R} \sin m\pi\frac{x}{L} \\
& \text{driven mode response} \\
& + B \sin(\omega t + \delta_b) \sin n\frac{y}{R} \sin m\pi\frac{x}{L} \\
& \text{companion mode response} \\
& + \epsilon\left\{\left[A^2+B^2\right]\left[C_1+C_3 \cos 2m\pi\frac{x}{L}\right]\right. \\
& \left. -\left[A^2\cos(2\omega t + 2\delta_a)-B^2\cos(2\omega t + 2\delta_b)\right]\left[C_2+C_4\cos 2m\pi\frac{x}{L}\right]\right\} \\
& \text{axisymmetric mode response} \\
& + \text{prismatic mode response} \\
& + \text{boundary layer terms and higher order terms}
\end{aligned}
\qquad (1)
$$

where A and B are the amplitudes of driven and companion mode responses respectively, δ_a and δ_b are phase angles associated with driven and companion modes, n is the number of full waves around the circumference of the shell, m is the number of half waves along the axis of the shell, and C_1 through C_4 are functions of the mode numbers m and n and the characteristics of the shell. The form of the response indicates that there will be both a driven and a companion mode response and also an axisymmetric response which will be proportional to the squares of the driven and companion mode responses.

The nature of the driven mode and companion mode response is determined by the frequency response relationship derived from the second order equations in ϵ. If the companion mode is not participating in the response, B = 0, then the frequency response relationship is given by

$$\left[(\Omega^2-1) + \left(\frac{h}{R}\right)^2 \frac{\alpha}{\lambda_o}\left(\frac{w_m}{h}\right)^2\right]^2 + \gamma^2\Omega^2 = \frac{G^2}{\lambda_o^2 \left(\frac{w_m}{h}\right)^2} \qquad (2)$$

where Ω is ω/ω_o (ω_o = linear resonant frequency from the zeroth order equations), $\lambda_o = \omega_o^2 (1-\nu^2) \frac{\rho R^2}{E}$, γ is a function of the damping, G is the forcing function amplitude, and α is a function of shell geometry and mode number.

Figure 3 is a plot of Eq. (2), for the specific shell parameters. The curve shows a softening type nonlinearity. The response jumps associated with this nonlinear behavior will occur along the vertical dashed lines depending on the direction in which the frequency is being changed.

The so-called backbone curve shown in Figure 3 is the free vibration response. The relationship for this curve may be obtained by setting G and γ equal to zero in (2). This produces:

$$\Omega^2 = 1 - \left(\frac{h}{R}\right)^2 \frac{\alpha}{\lambda_o}\left(\frac{w_m}{h}\right)^2 \qquad (3)$$

The parameter α determines the type of nonlinearity and the degree of nonlinearity of the driven mode response. As λ_o is always positive, the type of nonlinearity depends on the sign of α. For a hardening nonlinearity α is negative, for a softening nonlinearity α is positive. The degree of nonlinearity also depends on α. Figure 4 shows the value of the "nonlinearity parameter," $\left(\frac{h}{R}\right)^2 \frac{\alpha}{\lambda_o}$, for the various modes of vibration of the test specimen used in this work. Clearly the analysis indicates that either a hardening or a softening nonlinearity may occur, depending upon the mode of vibration excited.

In the event that the companion mode is participating in the response, the frequency response relationship is considerably more complex. Results for a specific case may, however, be obtained numerically. Figure 5 shows responses for the driven mode and the companion mode for a specific case. Both the response with and without companion mode participation are shown. Both curves represent possible responses of the shell. The actual response would have to be determined by a stability analysis. Clearly the companion mode will affect the driven mode response only in the vicinity of $\Omega = 1$.

Chen's analysis indicated further that the companion mode would only participate in the response if vibrations in the driven mode exceeded a certain amplitude.

This implies that the companion mode will participate only if the forcing amplitude is above a minimum value. This value depends on the specimen and the mode being studied. The results of Chen's analysis will be referred to throughout the discussion of the experimental results.

III. EXPERIMENTAL SETUP

The experimental setup is shown schematically in Figure 6 and pictorially in Figure 7. The test specimen, a thin aluminum shell, was vibrated with an induction vibrator. This vibrator applied an oscillating force in the radial direction to the surface of the specimen. A fibre optics probe was used to measure radial displacement. A detailed discussion of each of these components and their associated equipment follows.

3.1 Test Specimen

The test specimen was a thin-walled aluminum shell with the dimensions shown in Figure 8. A photograph of the specimen is provided in Figure 9. The shell material was aluminum alloy 6061 T6. It was manufactured from a seamless tube by first machining the inner diameter, expanding the tube thermally, mounting it on a steel mandrel and machining the outer diameter and end ring. The shell was removed from the mandrel by reheating the assembly.

The specimen was previously used in the experimental work by Chen (Ref. 12). At that time the thickness was measured accurately and found to vary no more than $\pm$ 4% from the mean at any point. In addition a scan of the shell shape was made using the apparatus developed by Arbocz and Babcock (Ref. 14). A plot of the shell imperfections is shown in Figure 10. The plot shows a maximum deviation from a perfectly cylindrical shape of approximately one half the thickness of the shell.

As shown in Figure 8 the shell includes integral end rings. These rings model the simple support boundary conditions. The

rings were designed based on the program developed by El Raheb (Ref. 15). The natural frequencies of the actual shell were compared to those of the modeled simply-supported shell (see Figure 11) and found to vary from predicted results by at most 9.16% for the modes studied in this work. Table I also shows this comparison.

The support plate for the specimen is shown in Figure 9. The shell rested on two O rings which placed a minimum restriction on the displacement of the shell. A few thousandths clearance was allowed for the interior O ring to insure that the motion of the shell was unimpeded. The support plate was mounted securely onto a large circular plate which also included the support mechanism for the probe. This in turn was bolted firmly to a square 1/4" thick plate which was in turn clamped onto a $1\frac{1}{2}$" steel plate, all of which insured that there would be no coupling between the vibrations of the shell and the support system which was essentially rigid.

3.2 Induction Vibrator

The induction vibrator circuit consisted of the vibrator itself and an audio amplifier and oscillator which provided the current for the vibrator. Two digital frequency counters were used to monitor the oscillator frequency and an ammeter was used to monitor the vibrator current.

The vibrator itself is shown schematically in Figure 12 and pictorially in Figure 13. The vibrator consisted of 2 magnets: a permanent doughnut magnet and an electromagnet mounted axially inside the doughnut magnet. The doughnut magnet had a steel end plate and an axial shaft which connected the core of the electromagnet

to the end plate. The shaft was threaded to allow adjustment of the electromagnet along the axis of the doughnut magnet. The field strength at the face of the doughnut magnet was approximately 1500 Gauss. The electromagnet consisted of approximately 300 turns of #30 copper wire about a laminated soft iron core. Additional hardware served to contain and direct the fields as shown.

Development work on the induction vibrator was done by Edgell and Rife (Refs. 16-18). Their work indicated that force obtained varied as the current in the electromagnet. For a detailed discussion of the principles involved the reader is referred to the work cited above. In short, the principle of operation is this.

The sinusoidal current in the electromagnet induces an oscillating magnetic field which permeates the specimen. As this field changes, due to a varying driving signal, eddy currents are generated in the specimen. These currents in turn produce a magnetic field which is then attracted or repulsed by the local pole of the permanent magnet. As the current in the electromagnet changes sign the direction of the eddy currents and hence their fields changes sign. An alternately pushing and pulling forcing function directly proportional to the electromagnet current results. Deviations from this simple picture occur because of the coupling effect of the eddy currents on the electromagnet. Because the field is not precisely symmetric lack of symmetry in the forcing function may result.

Several attempts were made to measure the force applied to the specimen. It was desirable to determine both the magnitude of the forcing function as it varied with current and the linearity of the

forcing function itself, or more explicitly how much it varied from a true sinusoid. The most successful attempt involved the suspension of an aluminum disc as a test specimen. A disc of the same thickness as the shell and of $1\frac{1}{2}$ inches outer diameter was suspended from four monofilament lines located symmetrically and under equal tension. It was possible to adjust the position of the disc independently along the three normal axes.

The induction vibrator was tested by vibrating the disc over a range of frequencies from 200 cps to 700 cps. This range was between the natural frequency of the suspended disc system and the lowest mode of the freely suspended disc itself. The displacement of the center of the disc was measured with an optical probe. Analysis of the resultant signal gave the data in Table II. Table II gives the components of the displacement signal for the first three harmonics at various vibrator frequencies and currents. The results show that the resultant displacement was composed in all cases of at least 93% driven frequency. This is a significant deviation from a perfect signal as this may lead to a larger fraction in the variation of the forcing function amplitude in the higher harmonics of the driven frequency. It is felt that these results may not, however, accurately reflect the behavior of the forcing function. The effect of acoustical damping, nonuniformities in the support of the disc and disc resonance frequencies may have affected the results. In addition, the frequency analyzer which was used to measure the relative amplitudes of the various components of the displacement signal was less accurate than desired. This is indicated by the fact that for certain of the measured

frequencies and currents the sum of the percentages of the first three harmonic components exceeds one hundred per cent.

Figure 14 shows the variation of the amplitude of the displacement with current for a given frequency, 600 cps. This result indicates that the amplitude of the oscillation of the disc, and hence the forcing function, varies linearly with current.

The forcing function magnitude was calculated for the various modes and currents studied. This calculation was based on the assumption that at the frequency observed, 600 cps, the disc responded as a freely suspended disc. The results of this computation are given in Table III. These magnitudes should be considered only as approximate values. Results will be presented in terms of induction vibrator current which is a directly measured quantity.

It was observed that a significant heating of the shell occurred due to the eddy currents. In order to minimize any effects this would have on the response of the shell, air flow was introduced through the base plate of the induction vibrator. The flow of air over the surface of the shell reduced the heating problem to a minimum and had no observable effect on the behavior of the specimen.

The exact area over which the forcing function acted, as well as the spatial distribution of the forcing function, is uncertain. The largest circumferential mode number studied was ten. This corresponds to a half wavelength on the surface of the shell of 1.26 inches. This was deemed sufficiently large compared to the size of the electromagnet core (.5 in.) to prevent significant destruction interference in the forcing of the various modes studied.

3.3 Photo Optical Probe

The displacement measuring device was an MTI fibre optics probe. The probe had a frequency response limit well above any of the frequencies at which the shell vibrated. Its linear range extended over approximately .055 inches, well over that required for the displacements observed. The probe had the further advantage of being unaffected by the oscillating magnetic field originating from the vibrator.

The probe had a diameter of 1/8". It was mounted exterior to the shell so that it could be adjusted circumferentially and axially. The ability to rotate the probe circumferentially was provided by the mount of the probe which consisted of a ring bearing that rotated around the specimen. The circumferential position of the probe could be monitored on the x axis of an xy plotter through a potentiometer circuit.

The RMS voltage of the probe was monitored directly with a Ballantine RMS meter. In addition a 2 channel oscilloscope provided a visual display of the probe output. The output could also be plotted as the y axis of the plotter referred to above. This gave a plot of displacement amplitude vs. circumferential position. This type of output was used primarily to identify modes and to locate maximums (antinodes) and minimums (nodes). A signal analyzer was employed to separate out the harmonic components of the displacement signal.

A typical calibration curve for the probe is shown in Figure 18. Note that a maximum output of 1 volt is shown. Due to the non-uniform reflectivity of the shell the probe had to be readjusted to this

maximum whenever its position was changed. Without this adjustment changes of up to $\pm$.1 volt could occur depending on the position. This was deemed unacceptable for general purposes and the probe was readjusted whenever it was moved. Ten separate calibration curves showed a variation in slope of no more than $\pm$2% about the mean, provided this readjustment was made.

In certain cases, however, it was necessary to scan the shell circumferentially to obtain meaningful data. This was necessary when a shift in nodal line position occurred. Data from the scan were than used. This method of obtaining results is described below. The nodal line shift phenomena will be discussed in detail in the results section. The source of data will be noted when applicable.

The normal method of taking data was to locate a node or antinode with the probe using the xy plotter. The probe was then adjusted and a frequency-amplitude test conducted, amplitude data being obtained from the Ballantine. When it was necessary to scan, the mean square displacement vs. circumferential position was plotted by the xy plotter. The plots were used as the source of measurement of amplitude. This latter technique was significantly less accurate and was employed only when necessary.

IV. RESULTS OF THE EXPERIMENTAL INVESTIGATION

Response in the vicinity of several separate modes of vibration was investigated. As each mode was unique in some fashion the results from each mode are discussed individually. A summary is then presented.

4.1 m = 1, n = 6 Mode

This was the most easily excited mode and the one in which the highest level of response could be obtained. It was primarily this mode that was investigated by Chen in his experimental work. In general the results are similar to his although certain significant discrepancies were noted. This mode is significant because it clearly demonstrated all of the nonlinear effects predicted by Chen's analysis.

The driven mode response indicated a strong softening behavior. The driven mode responses for two different excitation levels is shown in Figures 16 and 17. A jump phenomenon was observed in each case. As the frequency was increased the slope of the frequency-response curve approached the vertical. The response was unstable at this point and a jump to a higher value of displacement amplitude occurred. A decrease in frequency subsequent to the jump resulted in continued increase in displacement amplitude until a jump decrease occurred.

An increase in the amplitude of driven mode response was observed in the vicinity of the linearized natural frequency. This increase appears to be due to the participation of the companion mode in the vibration. One will notice that there are two curves

in Figures 16 and 17 in this vicinity. The lower curve reflects the data obtained from a stationary probe. The upper curve reflects data from scanned xy plots of the displacement amplitude. It was necessary to use this method in this vicinity due to a nodal line shift associated with the incidence of the companion mode participation.

The upper curve reflects the true maximum or antinodal value. In Chen's work nodal line shifts were not compensated for in this manner. His results do indicate, however, that such shifts did occur. This phenomenon would have gone unnoticed here had it not been for an apparent jump phenomenon in the companion mode at high smplitude. Since such high amplitudes were not attained in Chen's work there was no incentive for a careful check of nodal line location. The scanned data indicate that the effect of companion mode response on driven mode response is much higher than the stationary results shown. Indeed a significantly higher amplitude occurred than would have otherwise been observed.

Away from the region of companion mode response the nodal lines return to their original position. The stationary values of displacement are again accurate.

Chen's results are similar to the stationary probe data with one important exception. He observed a drifting phenomenon in the same region in which the companion mode effect was observed in this work. This phenomenon was not observed although amplitudes considerably higher than those observed by Chen were attained. It is believed that this drifting phenomenon may have been associated with the nodal line shift discussed above. It is also possible that

this phenomenon may have been due to lack of rigidity in the support system as substantial changes in this were made. Chen also observed a rotation of the shell itself at high amplitude. No such phenomenon occurred here. This is believed to have been due to eccentricity in the forcing function created by the acoustic driver employed by Chen or again due to a lack of rigidity in the support system.

The companion mode response for a stationary probe with i=0.5, 0.7 amps is shown in Figure 18. The response curve for i=0.7 indicates the apparent jump phenomenon which led to the discovery of the nodal line shift. Both response curves indicate a higher amplitude than that obtained by scanning the shell. Figure 19 shows the scanned data for i=0.7 for both the driven and companion modes. This superposition of the two modes of response indicates the effect of companion mode participation on the driven mode. Figure 20 shows similar data from another test. The two tests indicate a slight shift in the natural frequency of this mode. Such shifts were observed frequently in the results and are believed to be the result of small rotations of the shell or variations in the degree of cooling caused by the air flow induced over the shell. These shifts are a small fraction of the natural frequency and do not seem to qualitatively affect the results. Figure 21 shows the scanned companion mode and corresponding driven mode response for i = 0.5. The result here is similar to that of i=0.7 although at a lower amplitude.

An axisymmetric vibration at twice the driving frequency was observed in each mode to some extent. This response was

strongest for m = 1, n = 6. Results were obtained for that mode only. These are presented in Figure 22. The response which occurs at twice the driven frequency is similar in behavior to that of the driven mode. A similar degree of nonlinearity including a jump phenomenon was observed.

4.2 m = 1, n = 4

This mode showed an almost linear type of frequency response curve in the range of forcing function amplitudes investigated. As shown in Figure 23, however, a comparison of peak response for i =0.43 and i =0.53 indicates a slight softening behavior in the driven mode. In addition the location of ω_o also indicates that this is the case. No companion mode was observed for this vibration. Chen's theory indicates a strong softening behavior (Figure 4). This was not the case. It is possible that the approximations of shallow shell theory, including the neglect of inplane inertia, may not be valid for such a low circumferential mode number. A comparison of natural frequencies of the actual shell with those predicted by Donnell's linear theory (Figure 11) shows the greatest discrepancy of the modes studied for this mode. This will perhaps give rise to a discrepancy with results based on the shallow shell theory assumptions.

4.3 m = 2, n = 7

The m = 2, n = 7 mode shows a fairly strong softening nonlinearity in the driven mode (Figure 24). The data indicate no increase in amplitude in the vicinity of the linearized natural frequency, ω_o, as was the case with m = 1, n = 6. In fact no companion mode participation was observed at any of the forcing function amplitudes

tested. The softening behavior clearly becomes stronger with increased amplitude. A response at twice the natural frequency was observed but no quantitative results were obtained for that component. Chen's work indicates a softening nonlinearity of the same order as for m = 1, n = 6 (Figure 4). A comparison of m = 2, n = 7 at i = 0.45 to m = 1, n = 6 at i=0.5 shows very similar behavior in degree of nonlinearity.

4.4 m = 2, n = 8

This mode again showed a softening behavior in the driven mode. This mode was chosen for a detailed investigation of the growth in companion and driven modes with increase in amplitude of forcing function. Figures 25 and 26 show the results for driven and companion modes respectively for a wide variety of signal currents. The companion mode shows no shift in the location of the highest response from that of the linear natural frequency while the driven responses do show a shift. This is a result of the fact that companion mode data were taken in all cases under precisely the same conditions. Slight variations in shell position, pressure of cooling air and so on may have affected the results for the driven mode which were obtained over a span of several days. In spite of these shifts, the data clearly indicate the growth in nonlinearity of driven mode with forcing function and the growth in amplitude of both driven and companion modes.

The driven mode response indicates a clear softening nonlinearity even at the lowest amplitudes. For i=0.25, the lowest case for which a jump occurs, there is a distinct decrease in amplitude

just before the jump to lower amplitude with decreasing frequency.

The fact that such a decrease does not occur at any of the observed high amplitude jumps, in this or any other mode, indicates that the frequency response curve shape predicted by Chen is accurate in this sense (Figure 3).

The increase in driven mode response in the vicinity of the companion mode participation is observed for this mode also, particularly at higher amplitudes. No attempt was made to obtain scanned data in this case. This effect may therefore be slightly larger than the results show. The companion mode results indicated a clear, nearly linear type growth with current. Some companion mode participation was observed at even the lowest amplitudes investigated. Chen's work indicated that the companion mode occurred only at higher values, above some limiting value of forcing amplitude. This did not appear to be the case for this mode.

4.5 m = 2, n = 9

The m = 2, n = 9 mode was the most difficult to study because of the nodal shifts which occurred throughout the frequency response curve. This made it necessary to use scanned data throughout. The mode was deemed of sufficient importance, however, to sacrifice both time and accuracy in making an investigation, as this was the only mode that gave any evidence of a hardening type behavior.

Figure 27 shows the driven mode response for a stationary probe. The slight jump observed indicated a weak hardening behavior. An investigation of the scanned data indicates that in spite of the nodal shifts involved this is close to the correct shape.

Figure 28 shows one of four sets of data taken from the scans. The scatter of this data indicated the reduced accuracy of this technique. All four sets of scanned data, however, showed behavior within the scatter of each scan. They indicate as shown that the actual maximum occurs at the point of the jump phenomenon. This implies a true hardening type behavior. However investigation of the companion mode (Figure 29) reveals that the companion mode has a maximum in the vicinity of the jump and in fact experiences a jump itself at that point. The companion mode is associated with the linear frequency of vibration of the shell. Thus its maximum should, for a hardening nonlinearity, occur below the frequency at which maximum occurs for the driven mode. This was not the result here. This response has not been adequately explained. It did not arise due to any interaction with another mode and the phenomenon was repeatable. Chen's analysis does predict a strong hardening nonlinearity for this mode. This does not, however, seem to fully explain the nature of the response.

4.6 m = 2, n = 10

This was the highest n number studied. As shown in Figure 30 the driven mode response indicates a weak softening type nonlinearity. The growth with increased current indicates little or no shift to the left with increasing amplitude. The near vertical slope on the left side of the curve, however, is indicative of softening behavior, as is the location of ω_o. This behavior may be so weak that over the range of forcing functions studied no large shift in the frequency of the maximum response should occur. Although the

response curves are near vertical no jump phenomenon was observed. This mode is predicted by Chen to be strongly hardening. Again this was not the case. The unusual shape of the curve for i =0. 5 in the vicinity of the maximum is unexplained. No companion mode was observed for this mode.

4. 7 m = 1, n = 7, 8

The discussion of these modes has been postponed until last due to the fact that they display a behavior that has not been considered theoretically for the nonlinear vibrations of shells. This is the interaction that occurs when two modes are very close in frequency. In this case the difference in frequency was 3. 8 cps with n = 7 at 528. 0 cps and n = 8 at 524. 2 cps. As Figure 31 indicates the response-frequency behavior is quite complex.

As frequency is increased from below 510 cps the response is similar to any of the modes discussed so far. At 522. 2 cps, however, a jump occurs to a region in which a beating phenomenon takes place. Once beating has been initiated a change in frequency over the range from 521. 0 cps to 522. 6 cps will result in continued beating with a peak to peak variation as shown in Figure 31 of approximately 0. 2t. The beat frequency was 1. 66 cps. As the end of the beating region is approached the beat amplitude decreases. If frequency is decreased below 521. 0 cps a stable region is entered which extends to 519. 8 cps. A further decrease in frequency results in a jump down in amplitude to the level of response previously encountered. If frequency is decreased following this jump the beating region is reentered. It should be noted that the region of marginal

instability is evident in this region. A disturbance of the shell causes oscillations which occur at the beat frequency and either decay or grow to a maximum depending on the frequency. The smallest oscillations in the unstable region will develop rapidly to the maximum amplitudes shown in Figure 31. The observances of both an apparently stable response below the beat response and the beat response occurring at a higher amplitude is particularly notable.

An increase in frequency above the region of beating results in a continued increase in amplitude until another jump increase occurs at 524.6 cps. This jump was followed by behavior common to other softening modes previously discussed. The behavior below 527.2 was distinctly m = 1, n = 8, while that above 527.2 was distinctly m = 1, n = 7.

The response curve indicates that both modes are strongly softening. The beat phenomenon is of interest in that it was observed for no other modes, although certain others were quite close in frequency. For other mode pairs one of the two would dominate the response. This was observed for m = 2, n = 10 and m = 2, n = 11 which are only 6.5 cps apart. m = 2, n = 11 could be excited only at very low amplitudes when approached from above in frequency. The case here, however, shows a much stronger interaction.

4.8 Summary of Results

The nonlinear effects observed were in general those predicted by Chen. The greatest discrepancy with predicted behavior is the lack of any definitely hardening behavior in any of the modes at which it was predicted. These included (m = 2, n = 8), (m = 2, n = 9),

and (m = 2, n = 10). The driven mode response was softening with the exception of m = 2, n = 9, about which no definite conclusion can be drawn. Jump phenomena were observed for several modes. Magnitude of jumps increased with increase in forcing function and frequency of jumps decreased, in general, with increased amplitude.

The participation of strong companion mode response was observed in certain modes. It was observed that nodal line shifts occurred when the frequency was in the vicinity of the companion mode response frequency. Whether this is the result of shell imperfections or is a result of the ideal behavior of the shell could not be determined. The companion mode had the effect of increasing driven mode response when it was participating.

Axisymmetric response at $2\omega_n$ was observed to some degree in all the modes studied. This appears to be strongly related to the driven mode response as Chen's analysis predicts. Results for this mode show behavior exactly parallel to the driven mode behavior and approximately proportional to the square of the driven mode amplitude.

A strong interaction between adjacent modes was observed in one instance. This produced a beating phenomenon and a complex frequency response curve involving three separate jump phenomena.

V. CONCLUDING REMARKS

Although the existing theory compares favorably with the experimental results in that the predicted nonlinear effects were observed, it does not appear to adequately explain all of the phenomena observed.

The lack of any observable hardening mode is the most significant discrepancy with existing theory. Also the complex nature of the response of the companion mode as to when it does or does not participate is unexplained. The imperfect nature of any laboratory arrangement is certain to have an effect on the results. It is not felt, however, that the origin of such significant qualitative discrepancies may be found in these deviations from the mathematical model.

A beating instability may occur in the vibration of circular cylindrical shells provided two modes of vibration are close enough in frequency to one another. This instability may result in deflections well above those caused by the response of a single mode.

An important area for further experimental work is in the development of a highly accurate method for calibrating a non-contacting driving device. Exact comparisons with analytical results would be made possible by such a development.

To conclude, it would appear that, although significant progress has been made in the development of a theory for nonlinear cylindrical shell vibration, more progress will have to be made before the physical response of such shells is accurately predicted in all cases. The inclusion of such observed phenomena

as nodal line shifts and the effect of shell imperfections in the analysis would facilitate such a comparison. It is hoped that this work will provide a basis for comparison with any further progress.

REFERENCES

1. Olsen, M. D. and Fung, Y. C., "Supersonic Flutter of Circular Cylindrical Shells Subjected to Internal Pressure and Axial Compression." AIAA J., vol. 4, no. 5, May 1966, pp. 858-864.

2. Reissner, Eric, "Nonlinear Effects in the Vibrations of Cylindrical Shells." Report No. AMS-6, Guided Missile Res. Dir., Ramo-Wooldridge Corp., Sept. 30, 1955.

3. Chu, Hu-Nan, "Influence of Large Amplitudes on Flexural Vibrations of a Thin Circular Cylindrical Shell." J. Aerospace Sci., vol. 28, no. 8, Aug. 1961, pp. 602-609.

4. Cummings, B. E., "Some Nonlinear Vibration and Response Problems of Cylin rical Panels and Shells." SM 62-32 (AFOSR 3123) Graduate Aero. Labs., California Institute of Technology, June 1962.

5. Nowinski, J. L., "Nonlinear Transverse Vibrations of Orthotropic Cylindrical Shells." AIAA J., vol. 1, no. 3, March 1963, pp. 617-620.

6. Evensen, D. A., "Nonlinear Flexural Vibrations of Thin-walled Circular Cylinders." NASA TN D-4090, Aug. 1967.

7. Dowell, E. H. and Ventres, C. S., "Model Equations for the Nonlinear Flexural Vibrations of a Cylindrical Shell." International Journal of Solids and Structures, voo. 4, no. 6, June 1968, pp. 975-991.

8. Matsuzaki, Y. and Kobayashi, S., "An Analytical Study of Nonlinear Vibration of Thin Circular Shells." Journal of Japan Society for Aeronautical and Space Sciences, vol. 17, no. 187, pp. 308-315, 1969.

REFERENCES (Cont'd)

9. Matsuzaki, Y. and Kobayashi, S., "A Theoretical and Experimental Study of the Nonlinear Flexural Vibration of Thin Circular Cylindrical Shells with Clamped Ends." Japan Society for Aeronautical and Space Sciences, vol. 12, no. 21, 1969.

10. Mayers, J. and Wrenn, B. G., "On the Nonlinear Free Vibrations of Thin Circular Cylindrical Shells," SUDAAR 269, June 1966, Dept. of Aeronautics and Astronautics, Stanford Univ.

11. Bleich, H. H. and Ginsberg, J. H., "Nonlinear Forced Vibrations of Infinitely Long Cylindrical Shells." Technical Report No. 46, Contract Nonr-266186, Dept. of Civil Engineering and Engineering Mechanics, Columbia University, Nov. 1970.

12. Chen, Jay-Chung, "Nonlinear Vibrations of Cylindrical Shells." Ph.D. Thesis, California Institute of Technology, Dec. 14, 1971.

13. Olsen, M. D., "Some Experimental Observations on the Nonlinear Vibration of Cylindrical Shells," AIAA J., vol. 3, no. 9, Sept. 1965, pp. 1775-1777.

14. Arbocz, J., and Babcock, C. D., "The Effect of General Imperfections on the Buckling of Cylindrical Shells." Journal of Applied Mechanics, vol. 36, no. 1, March 1969, pp. 28-38.

15. El Raheb, M., "Some Approximations in the Dynamic Shell Equations," Ph.D. Thesis, California Institute of Technology, Dec. 1, 1969.

16. Edgell, A. D. and Rife, D. O., "Preliminary Theoretical Investigation of the Induction Shaker." TM 398-22, 1-1, Convair Division of General Dynamics Corp., June 5, 1959.

REFERENCES (Cont'd)

17. Edgell, A. D. and Rife, D. O., "Experimental Test of the Induction Vibrator." TM 348-22, 1-2, Convair Division of General Dynamics Corp., September 22, 1959.

18. Edgell, A. D. and Rife, D. O., "Induction Vibration Equipment Development." ERR-PO-026, Convair Division of General Dynamics Corporation, Nov. 4, 1960.

TABLE I

Comparison of Measured Natural Frequencies to Computed

m = 1

n	ω_e	ω_o	E
4	973.2	1069.4	9.01
6	589.8	558.1	5.68
7	528.0	486.1	8.63
8	524.2	488.1	7.43

m = 2

n	ω_e	ω_o	E
7	1404.0	1378.69	1.98
8	1202.6	1148.21	4.73
9	1083.2	1014.93	6.73
10	1029.1	963.23	6.84

ω_e = observed value of natural frequency (cps)

ω_o = calculated valve based on Donnell's approximation (cps)

$$E = \frac{|\omega_o - \omega_e|}{\omega_o} \times 100$$

TABLE II

Results of Disc Tests

ω_i	i	ω_o	%
208	0.675	208	98.0
		416	0.05
		624	0.01
304	0.70	304	100.0
		608	4.0
		912	0.85
417	0.68	417	95.0
		834	5.0
		1251	1.5
600	0.3	600	95.0
		1200	1.6
		1800	1.3
600	0.4	600	94.0
		1200	2.2
		1800	3.0
600	0.5	600	94.0
		1200	2.7
		1800	3.8
600	0.6	600	95.0
		1200	6.5
		1800	4.7

TABLE II (Cont'd)

ω_i	i	ω_o	%
700	0.4	700	94.0
		1400	3.6
		2100	2.3
700	0.5	700	93.0
		1400	4.2
		2100	3.0
700	0.6	700	93.0
		1400	8.0
		2100	5.0

ω_i = oscillator frequency, cps

i = signal current, rms amps

ω_o = displacement component frequency

% = displacement component percentage

TABLE III

Forcing Function Amplitude

m	n	i amps	f, lbs
1	6	0.5	0.20
		0.7	0.27
1	4	0.43	0.17
		0.53	0.21
2	7	0.25	0.10
		0.35	0.14
		0.45	0.18
2	8	0.10	0.04
		0.15	0.06
		0.20	0.08
		0.25	0.10
		0.30	0.12
		0.35	0.14
		0.40	0.16
		0.45	0.18
2	9	0.45	0.18
2	10	0.30	0.12
		0.40	0.16
		0.50	0.20
1	7	0.60	0.24
1	8	0.60	0.24

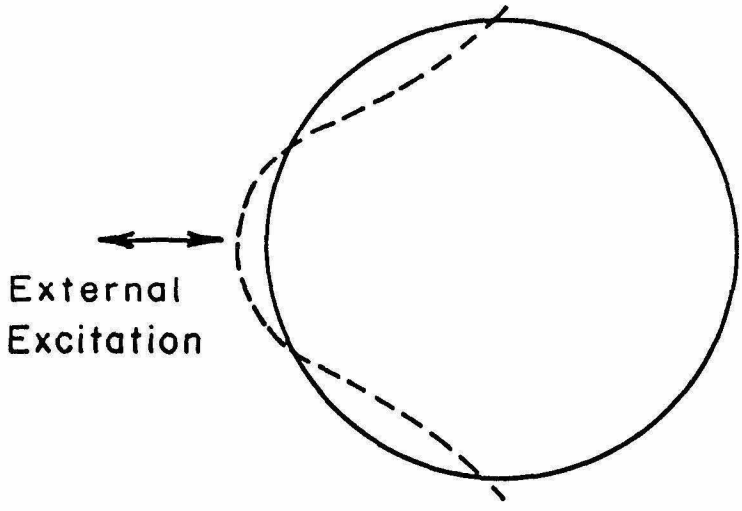

Driven Mode

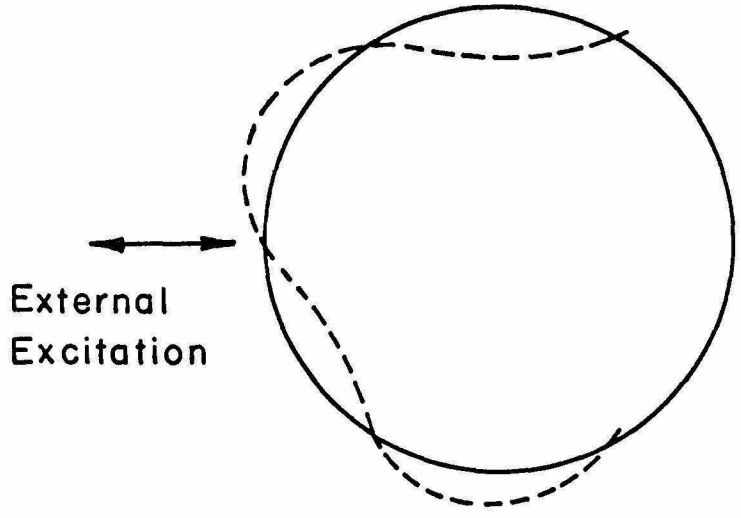

Companion Mode

FIG. 1 DRIVEN AND COMPANION MODES

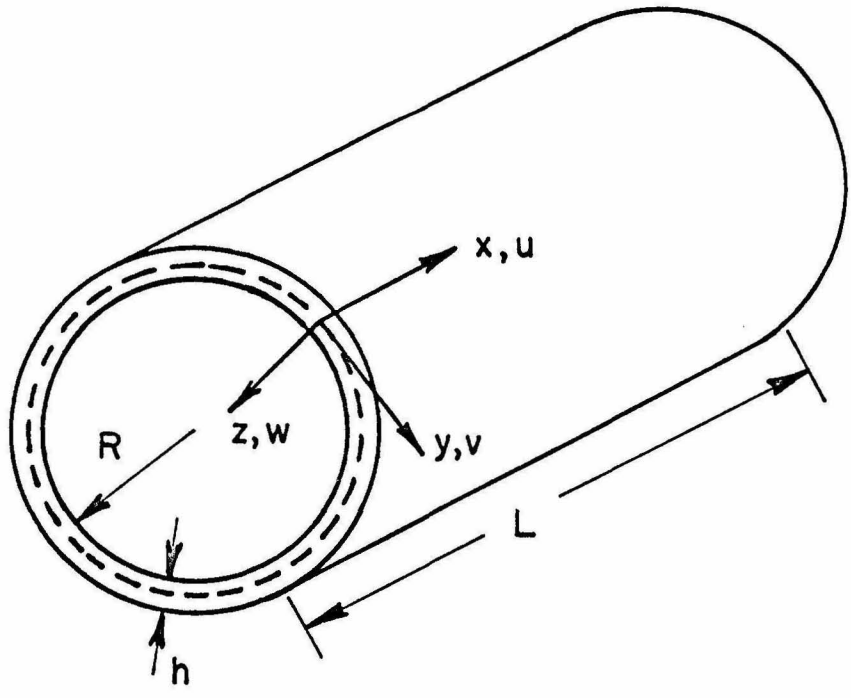

FIG. 2 SHELL GEOMETRY AND COORDINATE SYSTEM

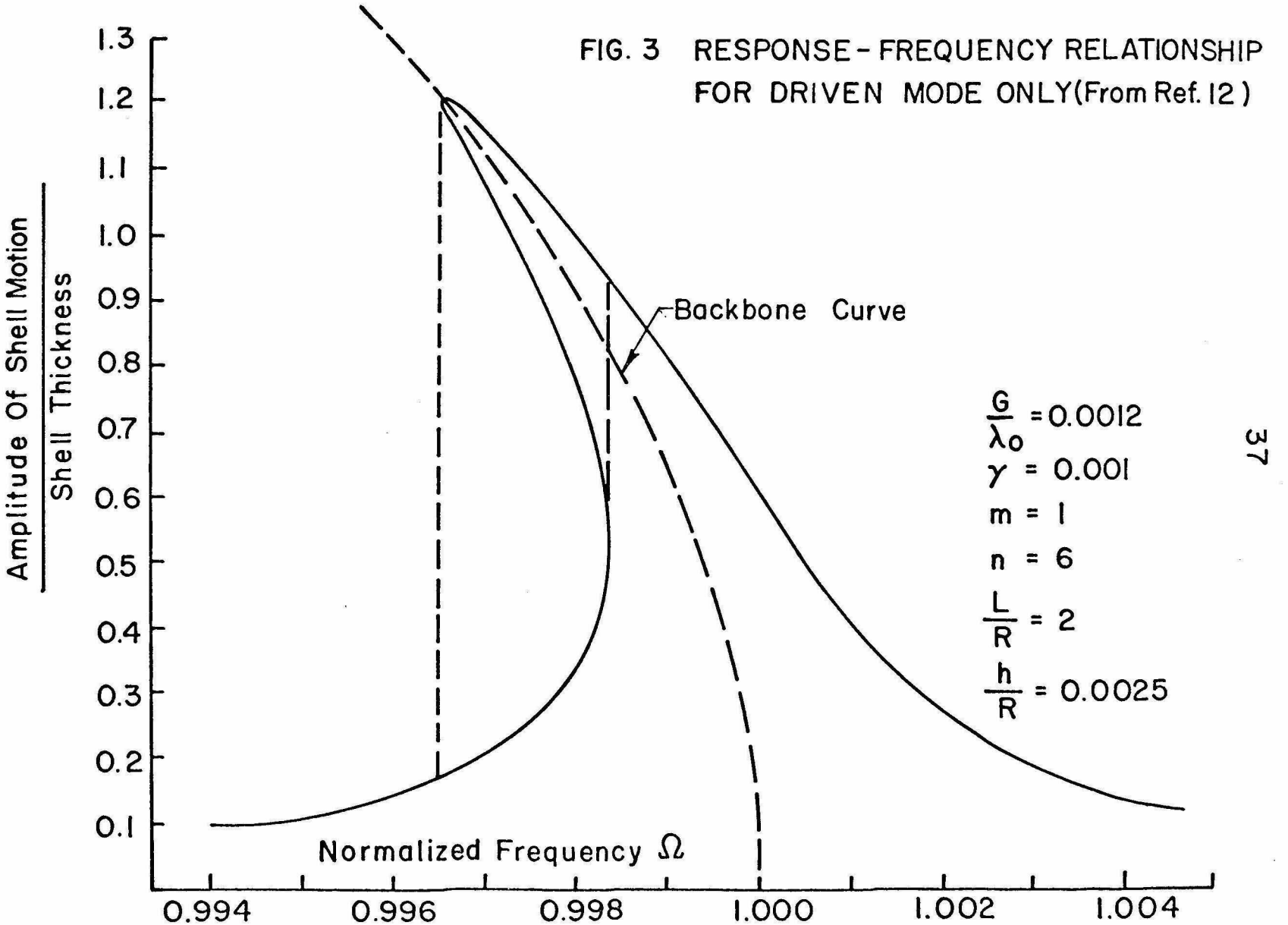

FIG. 3 RESPONSE - FREQUENCY RELATIONSHIP FOR DRIVEN MODE ONLY (From Ref. 12)

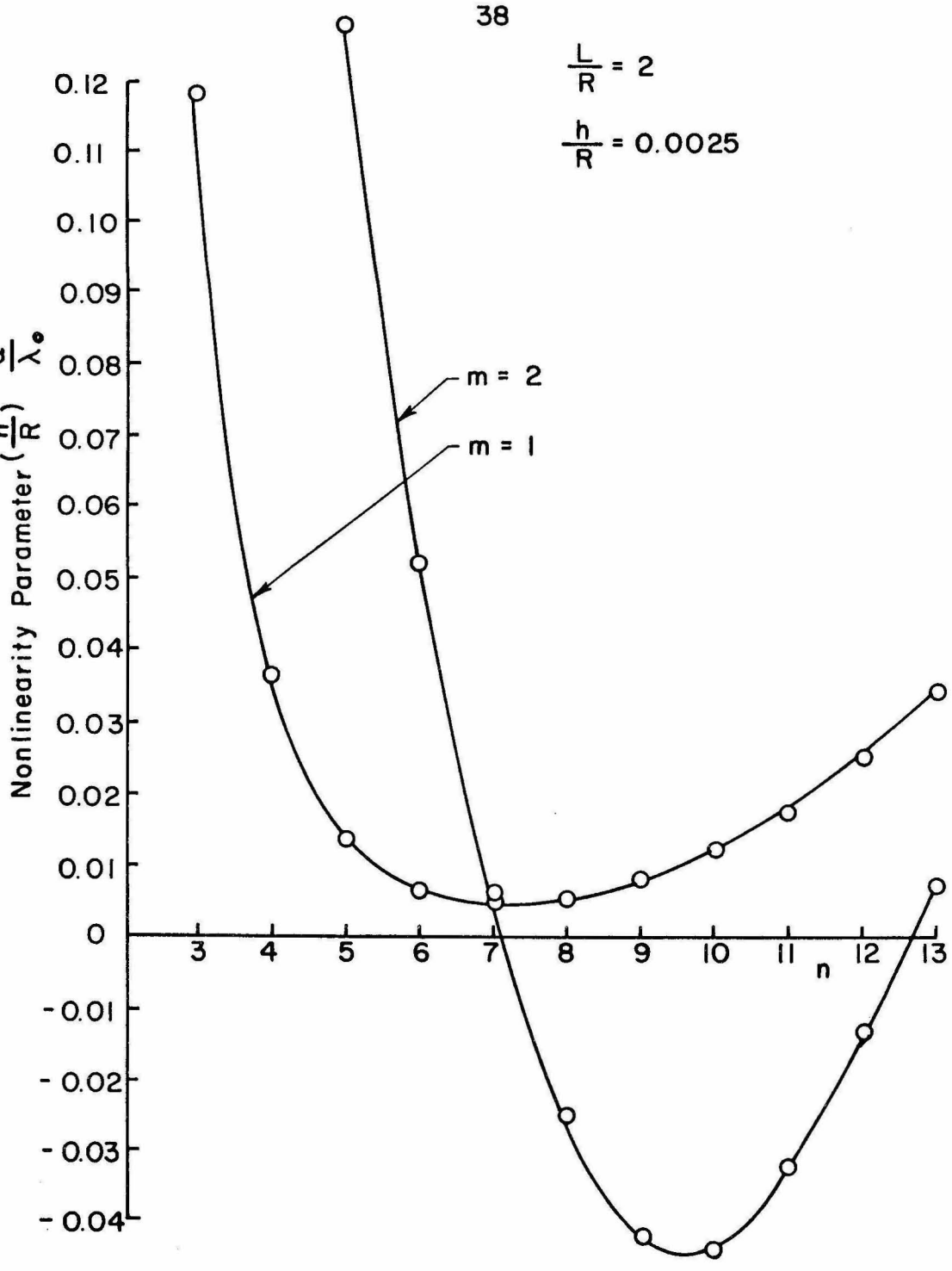

FIG. 4 NONLINEARITY PARAMETER (From Ref. 12)

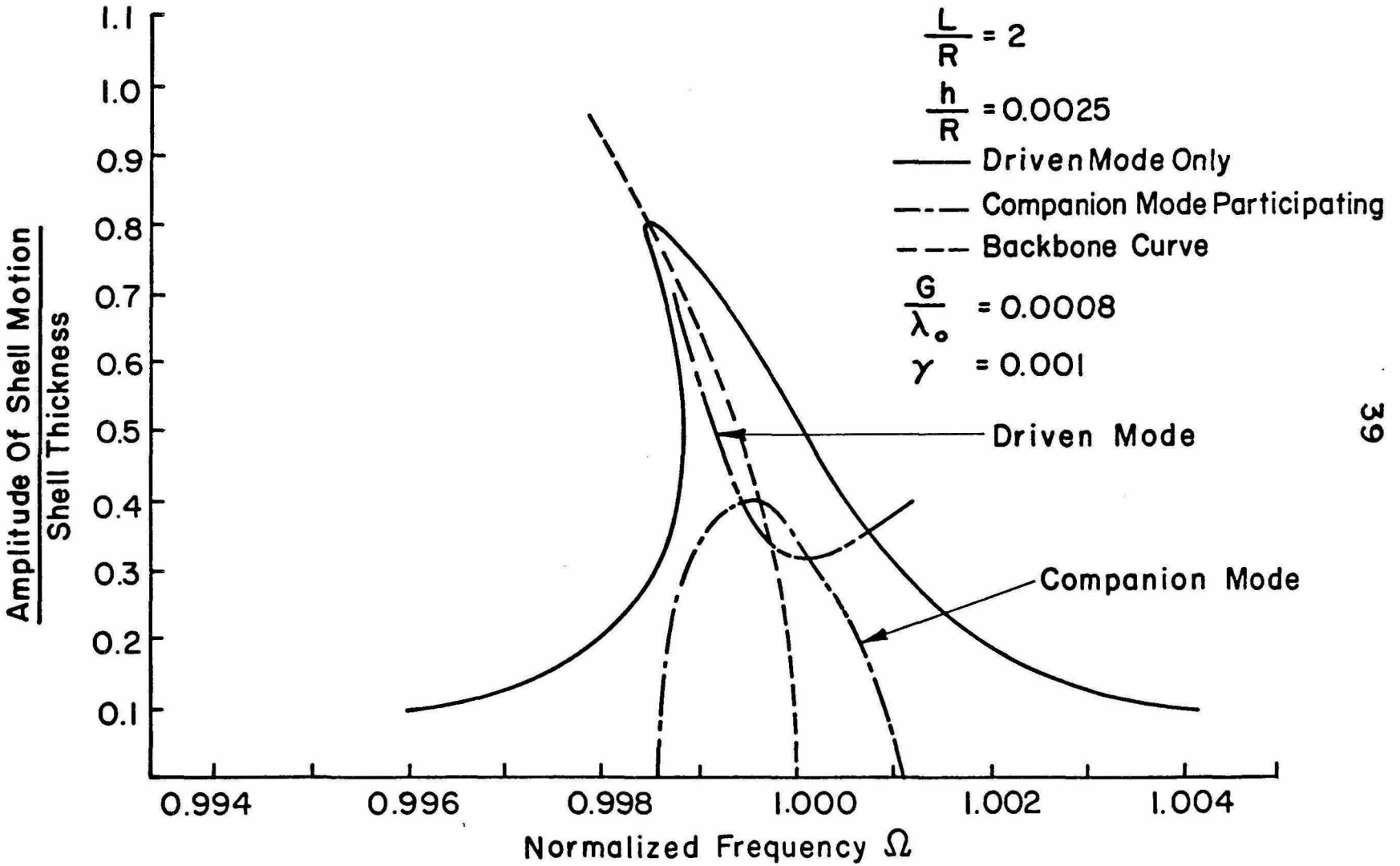

FIG. 5 RESPONSE-FREQUENCY RELATIONSHIP FOR MODE m=1, n=6 (From Ref. 12)

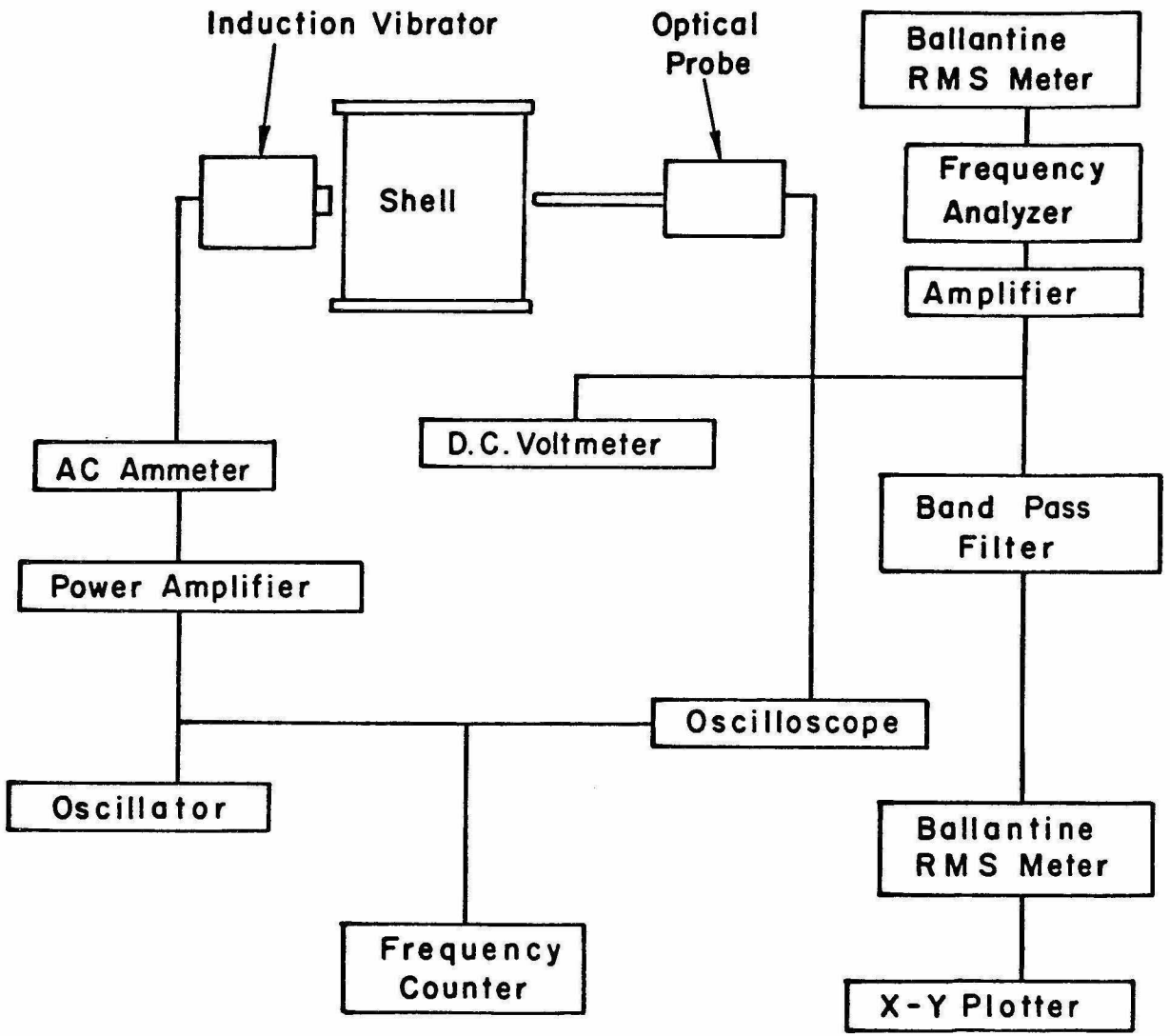

FIG. 6 SCHEMATIC OF EXPERIMENTAL SET UP

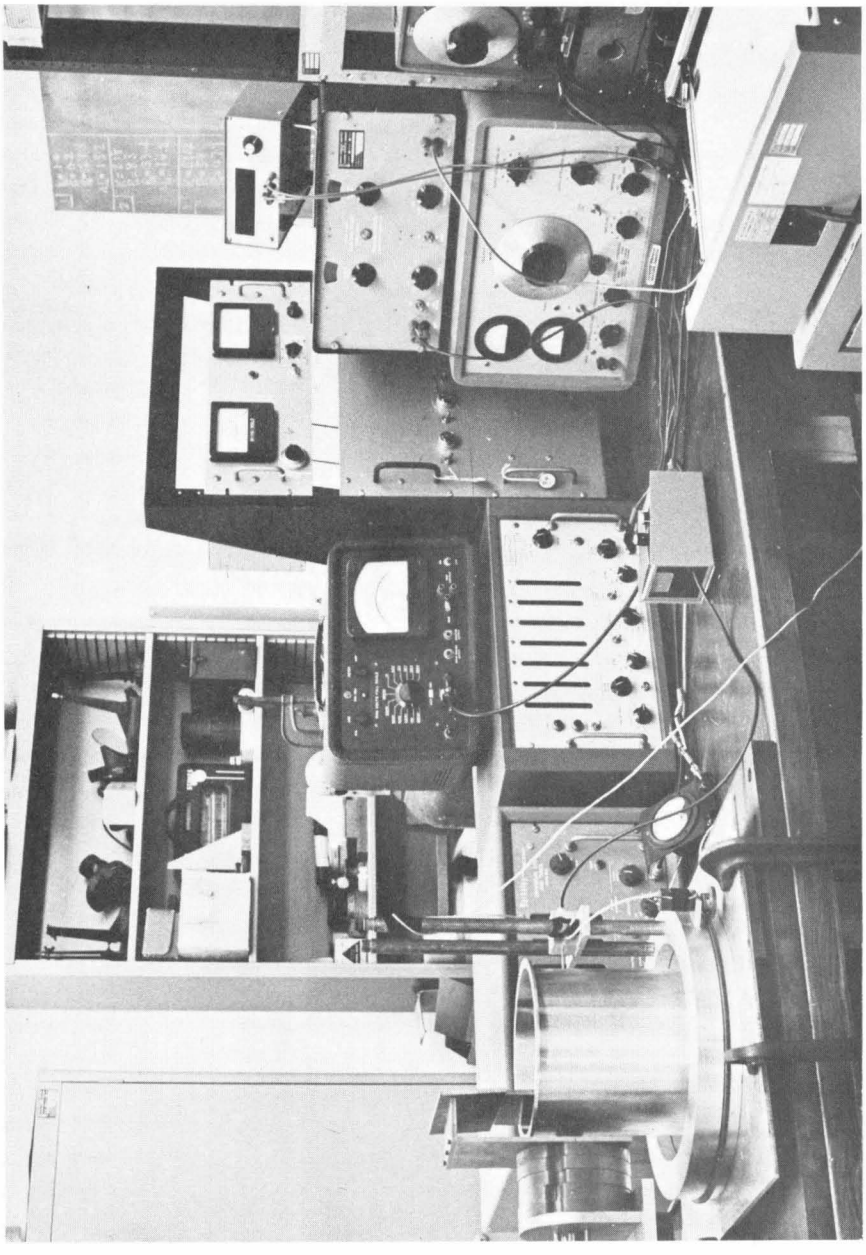

FIG. 7 EXPERIMENTAL SET UP

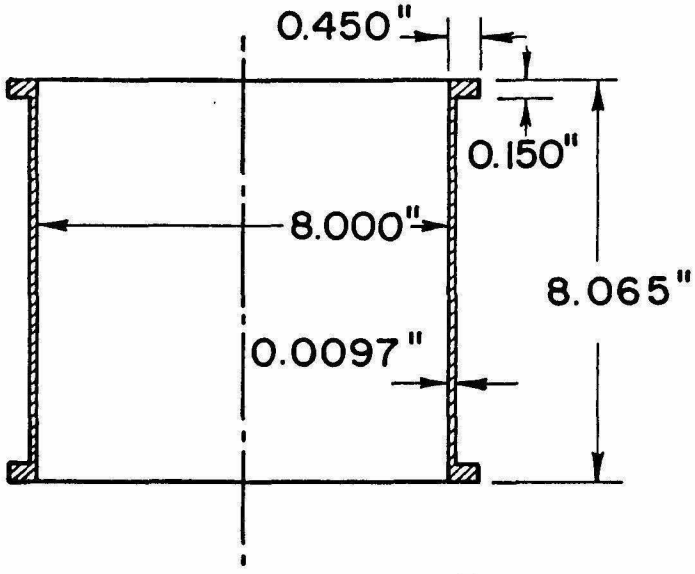

Density, $\rho = 0.101$ lb./in.^{3}

Young's Modulus, $E = 10.3 \times 10^6$ psi

Poisson's Ratio, $\nu = 0.31$

FIG. 8 PROPERTIES OF SHELL-RING SPECIMEN

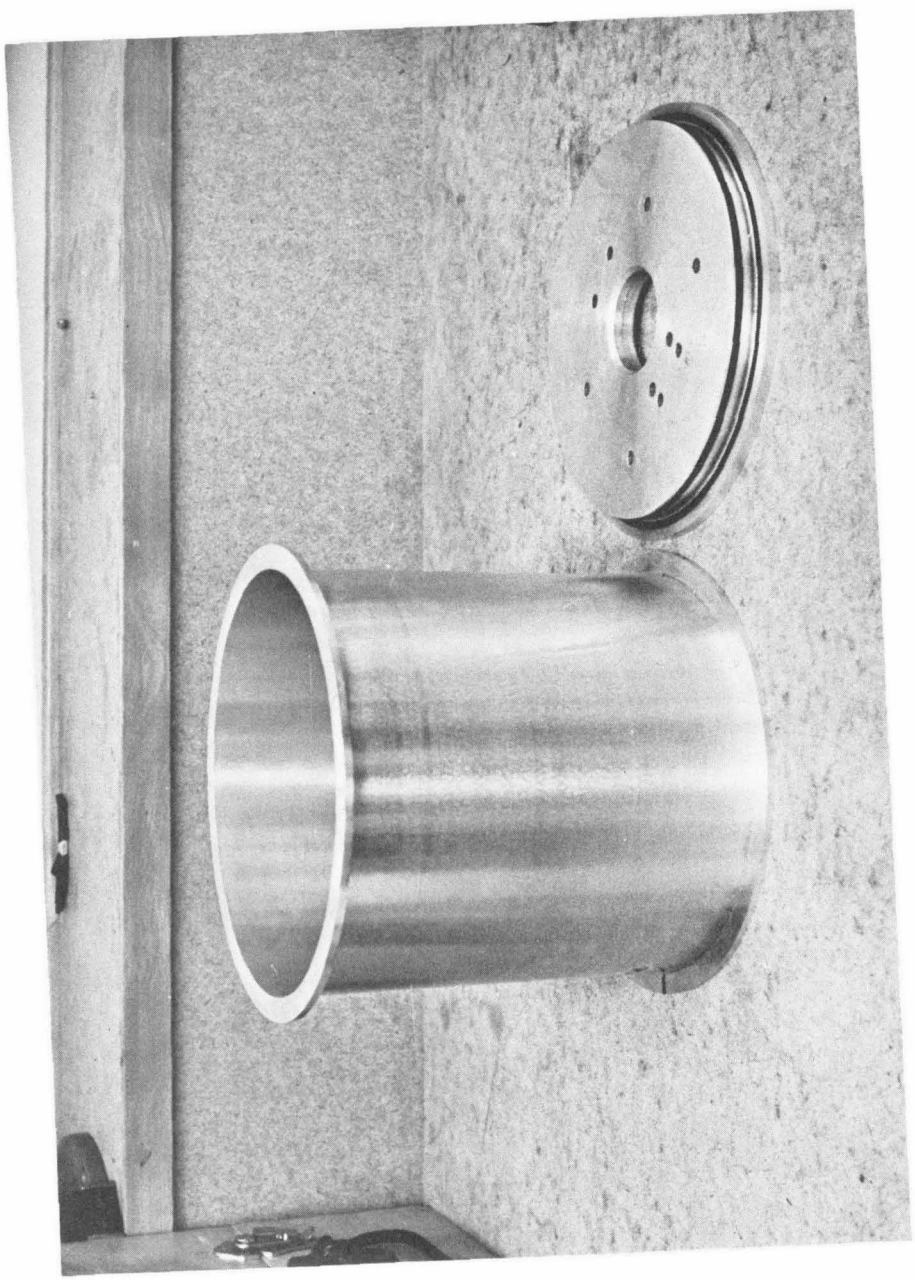

FIG. 9 TEST SPECIMEN AND SUPPORT PLATE

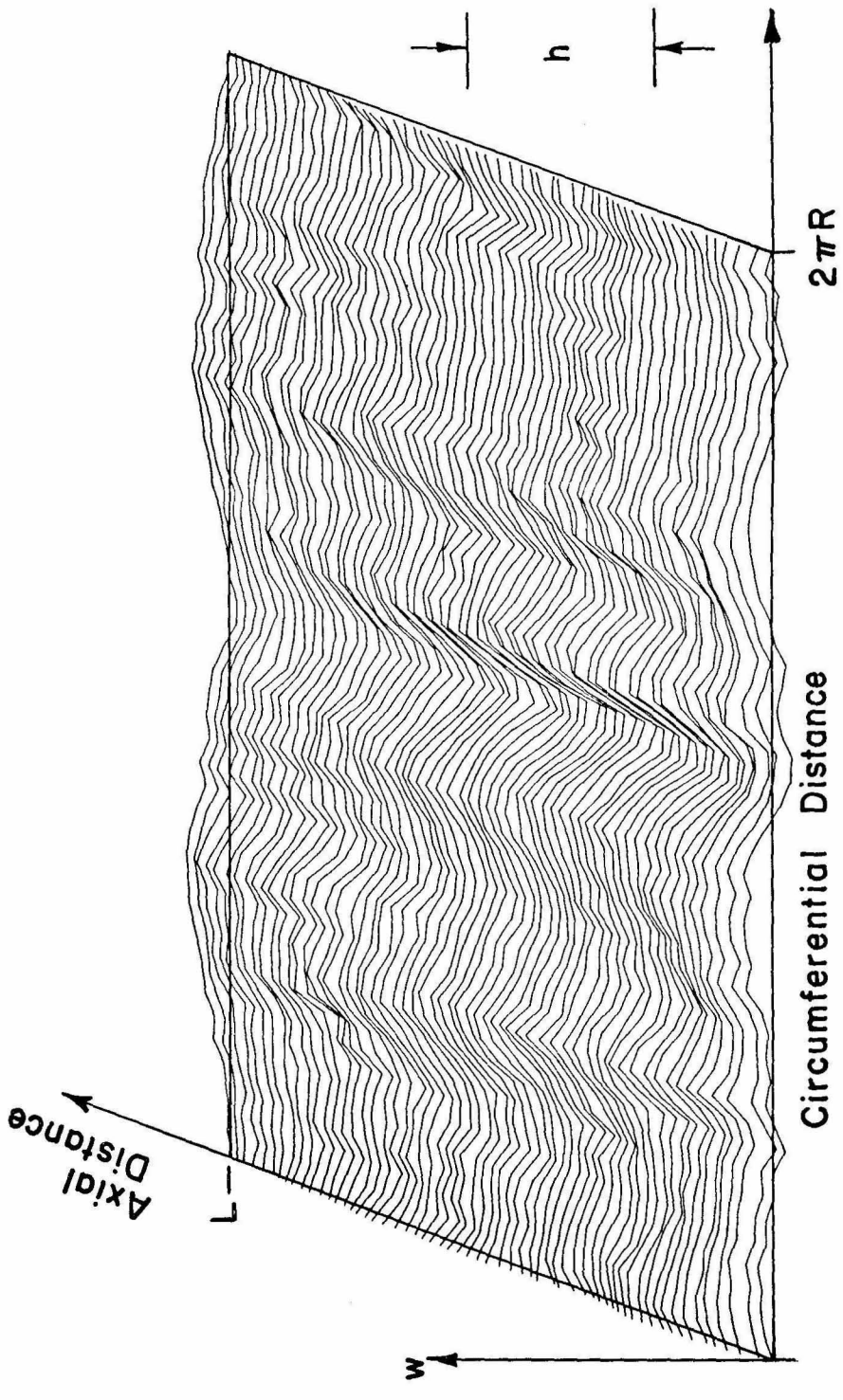

FIG. 10 SHELL IMPERFECTIONS

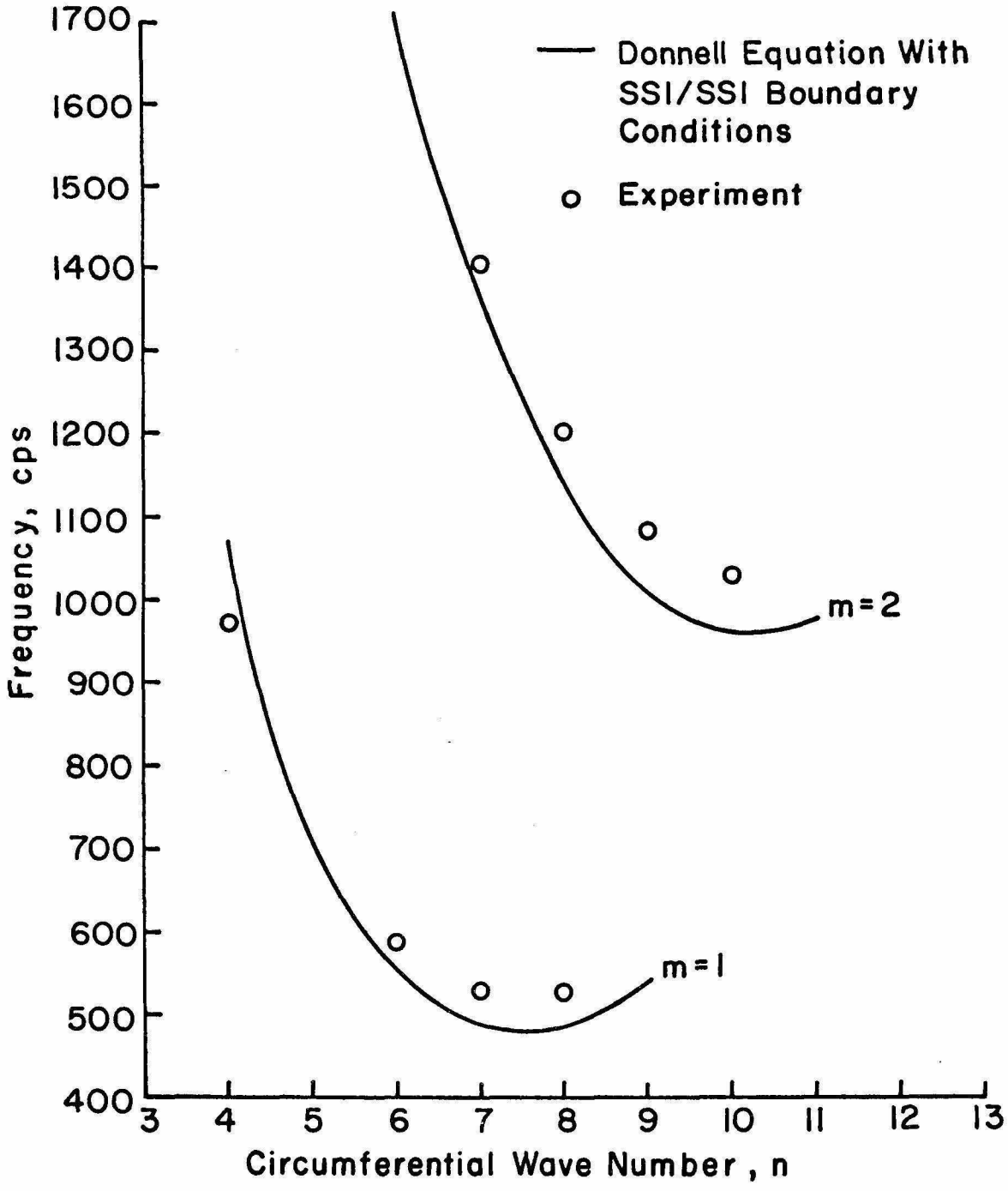

FIG. 11 FREQUENCY SPECTRUM OF SHELL SPECIMEN

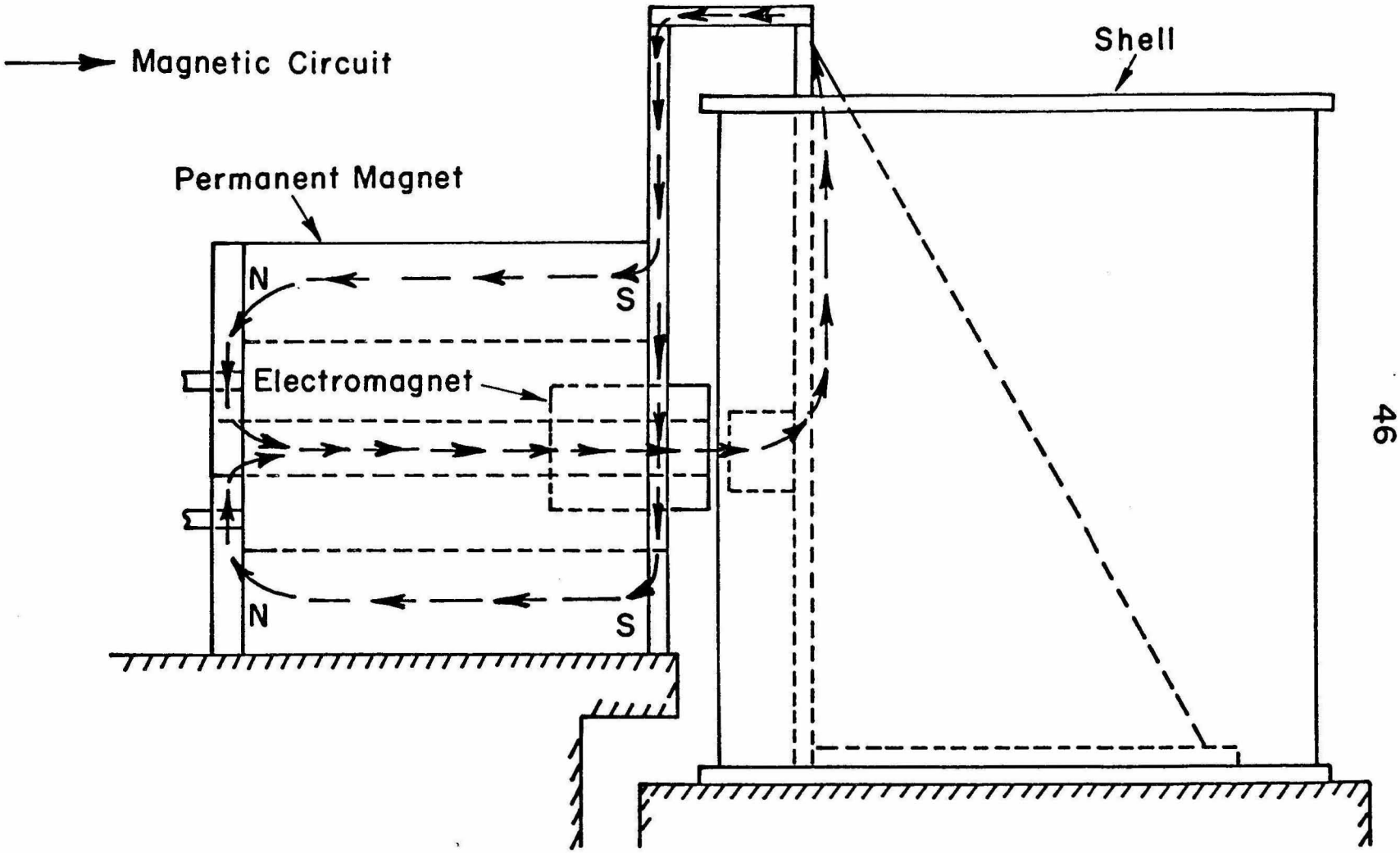

FIG. 12 SCHEMATIC OF INDUCTION VIBRATOR

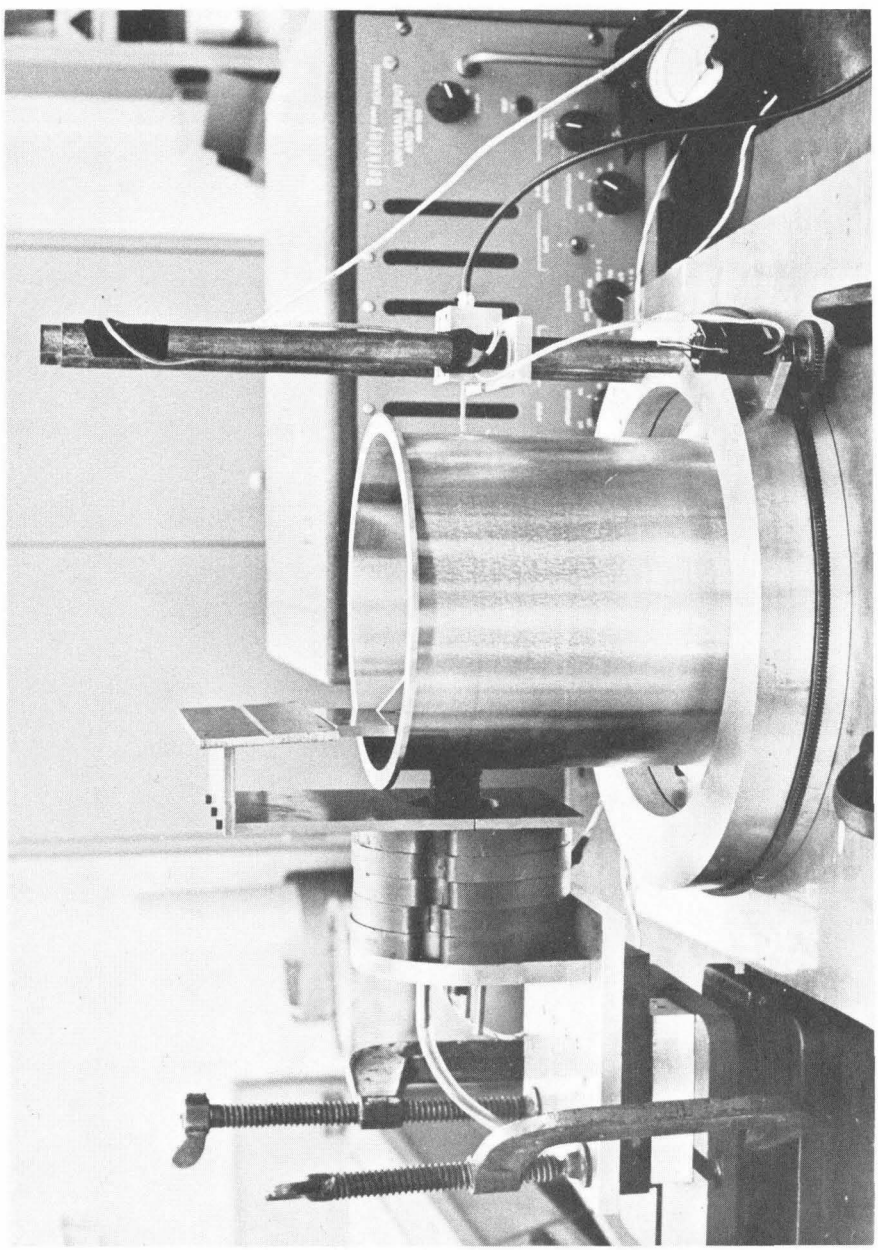

FIG. 13 INDUCTION VIBRATOR AND CONFIGURATION

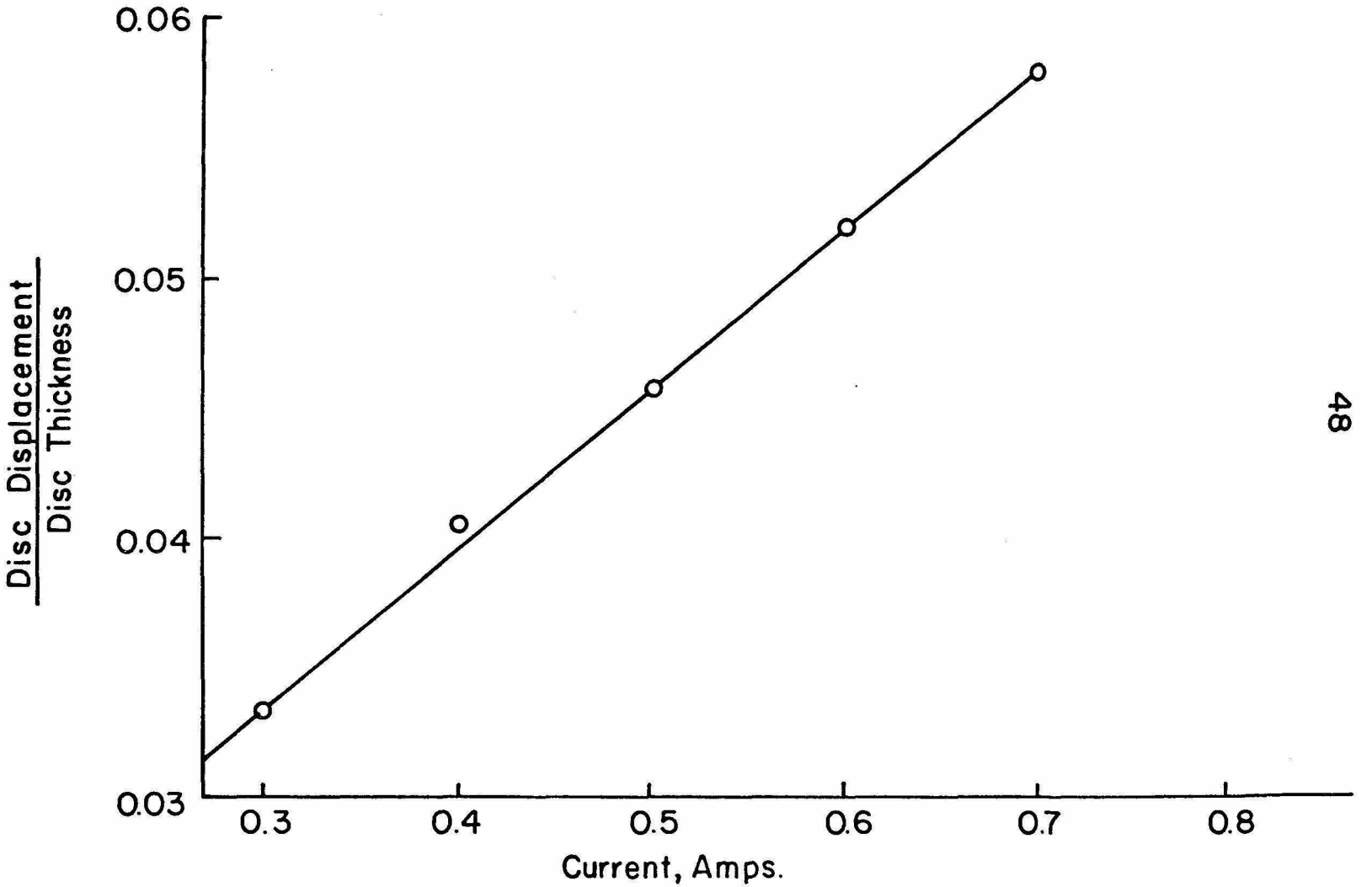

FIG. 14 INDUCTION VIBRATOR CURRENT VS DISC DISPLACEMENT AT 600 CPS

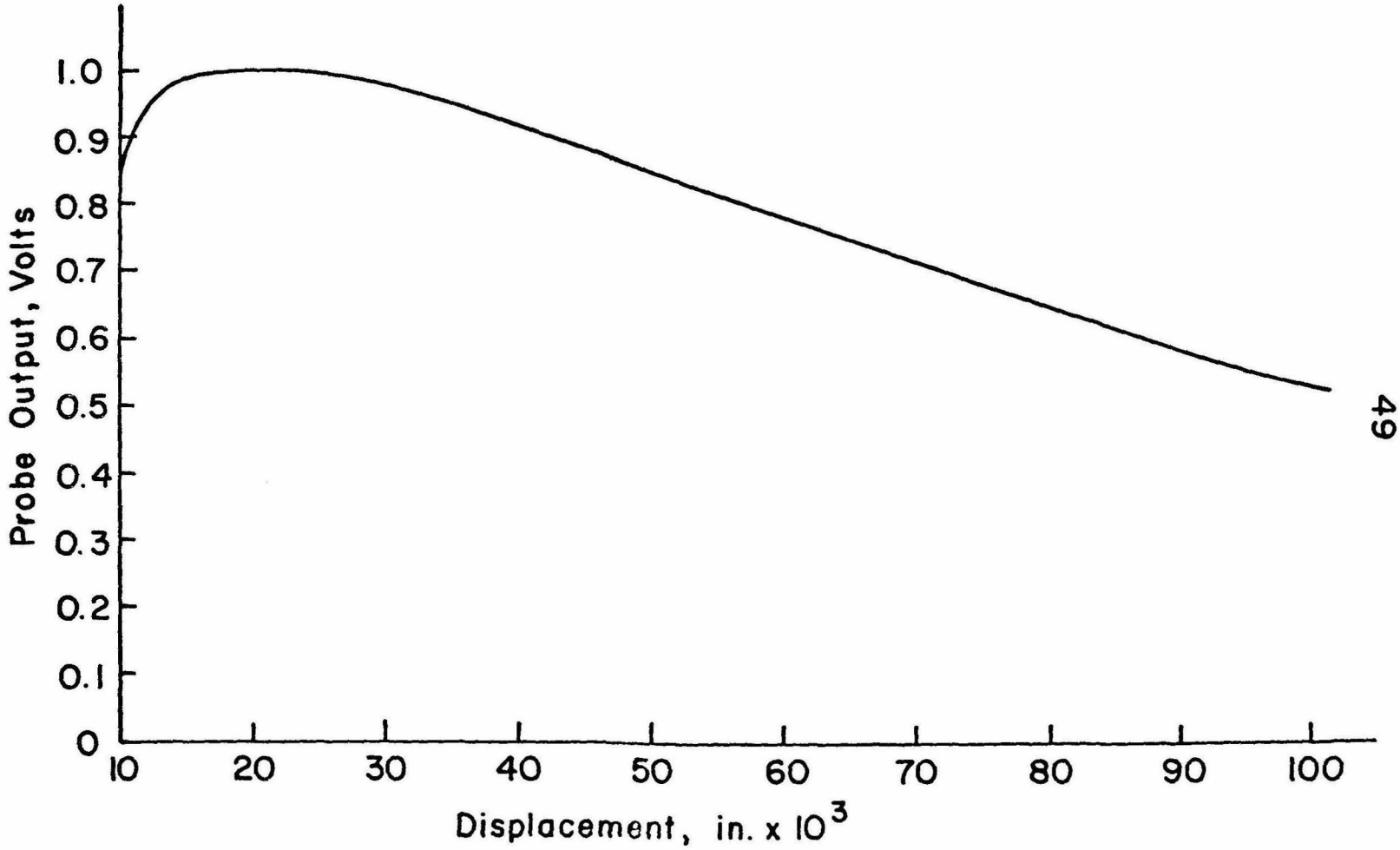

FIG. 15 CALIBRATION OF FIBRE OPTICS DISPLACEMENT TRANSDUCER

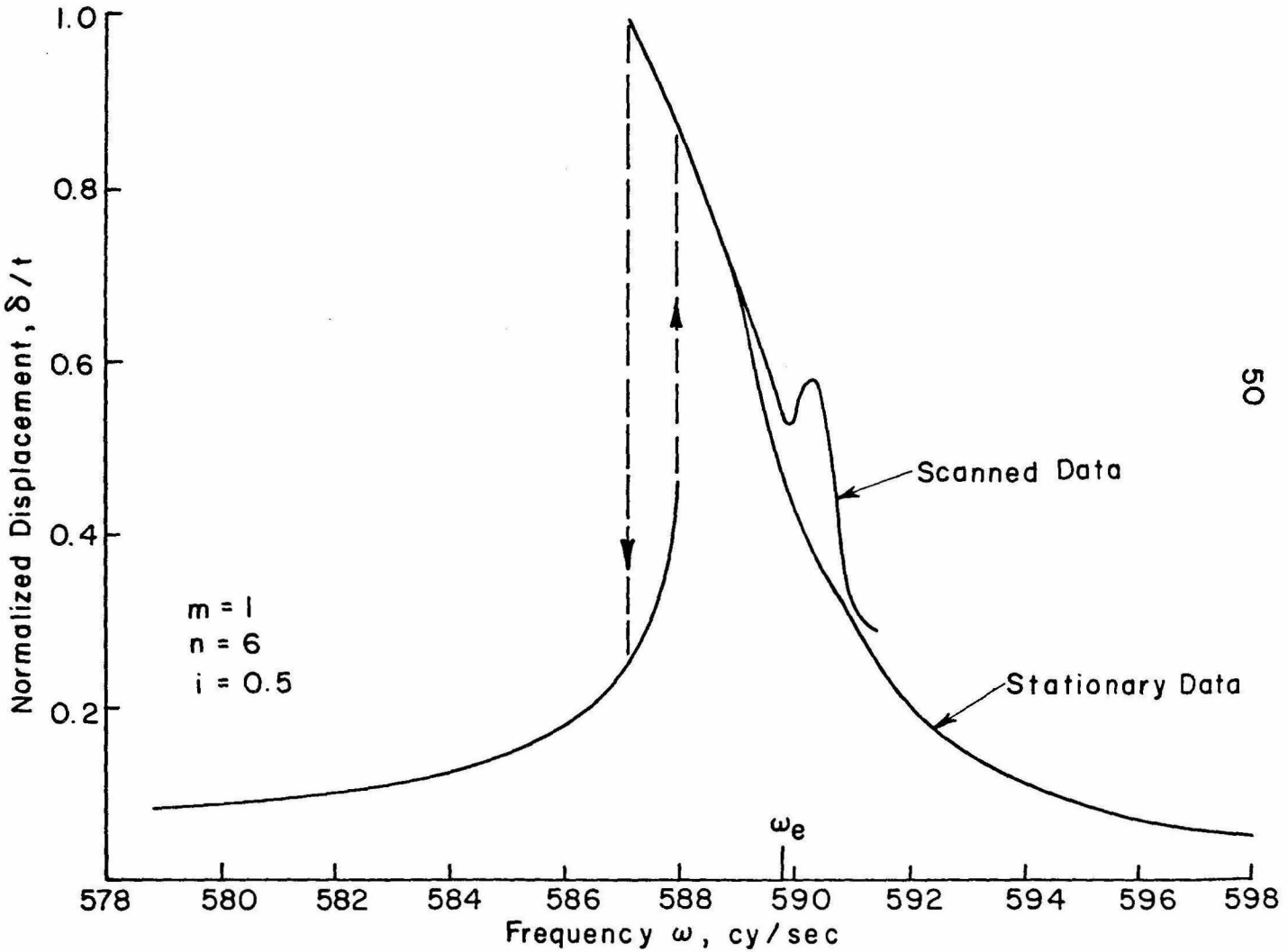

FIG. 16 DRIVEN MODE RESPONSE

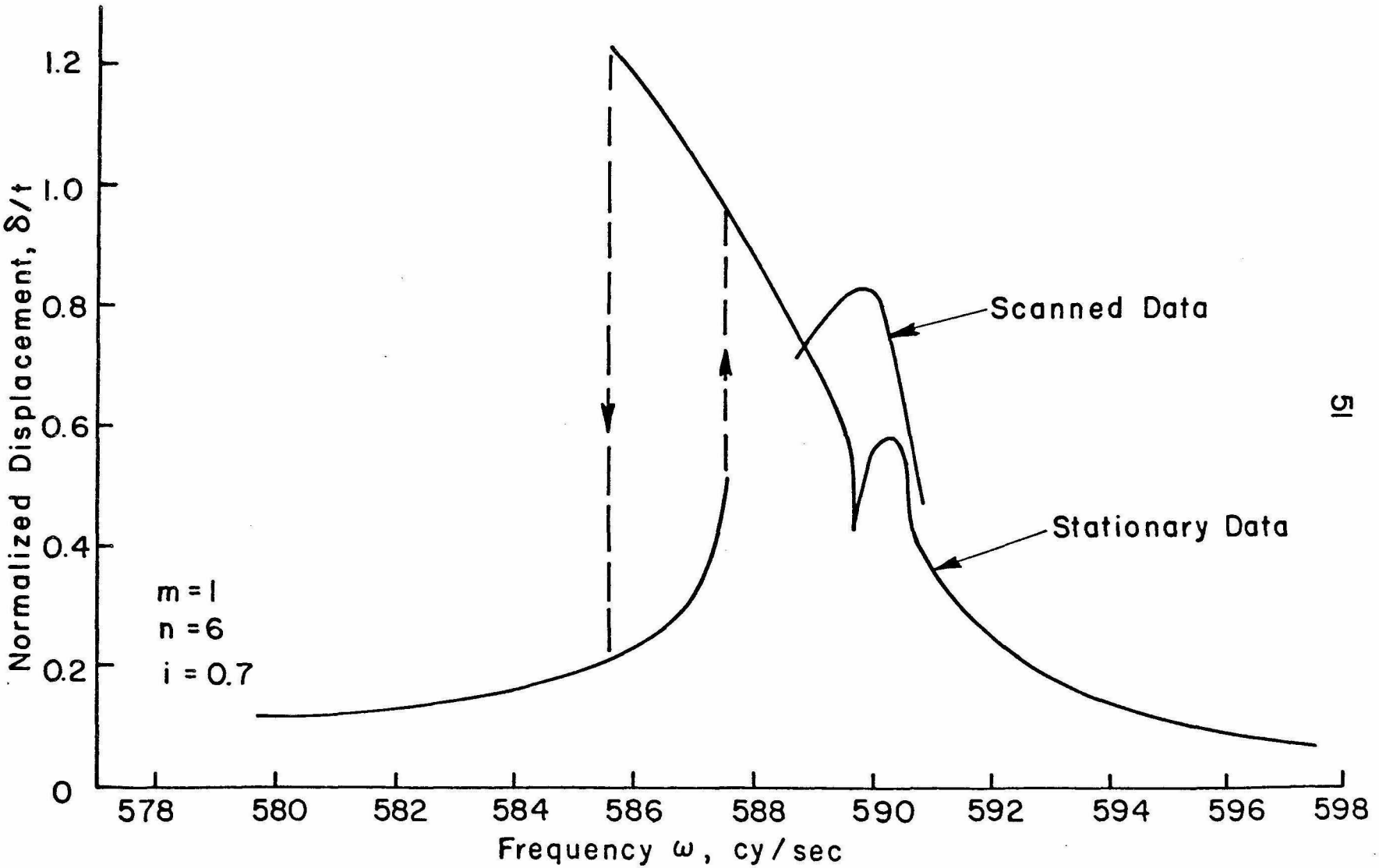

FIG. 17 DRIVEN MODE RESPONSE

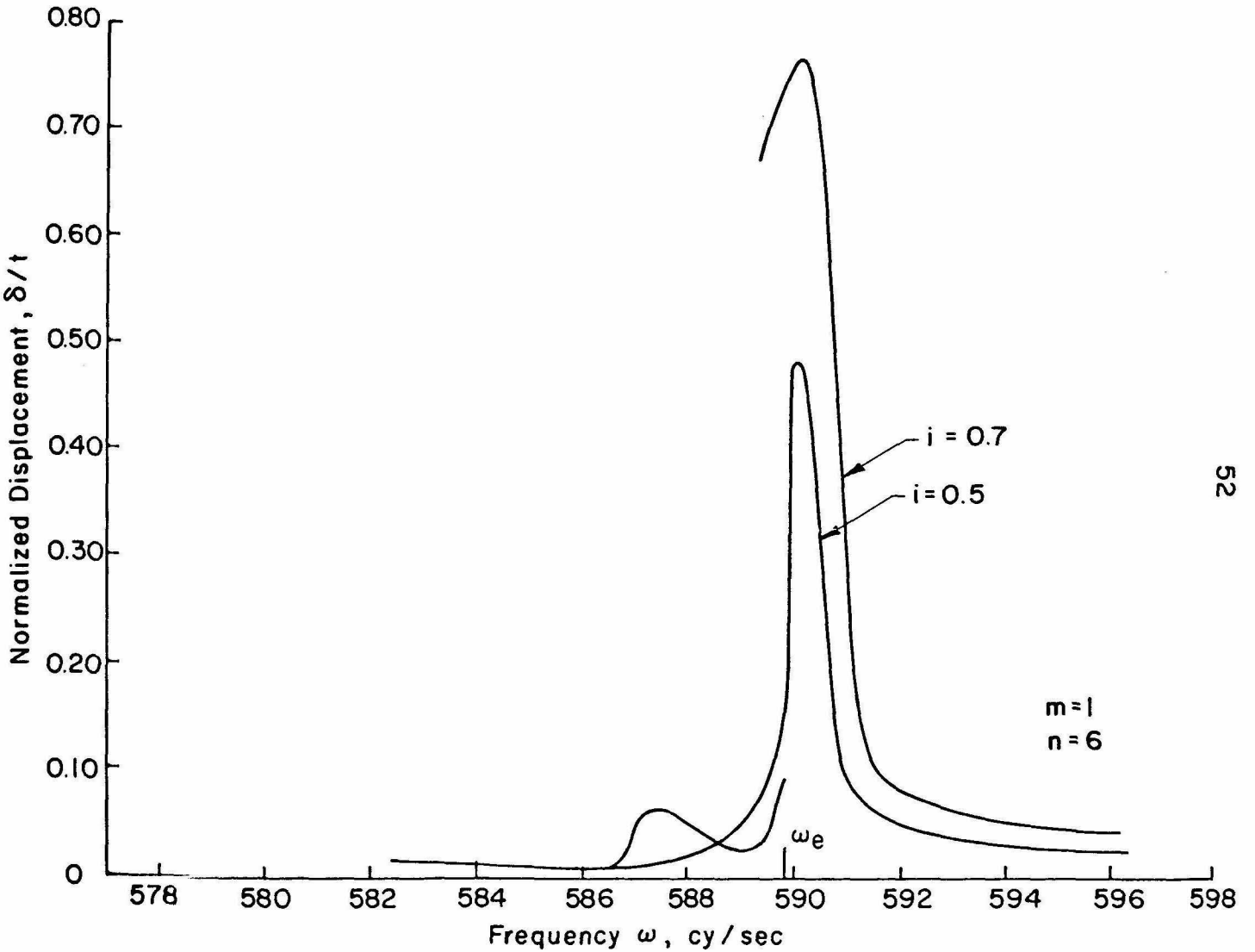

FIG. 18 COMPANION MODE RESPONSE, STATIONARY DATA

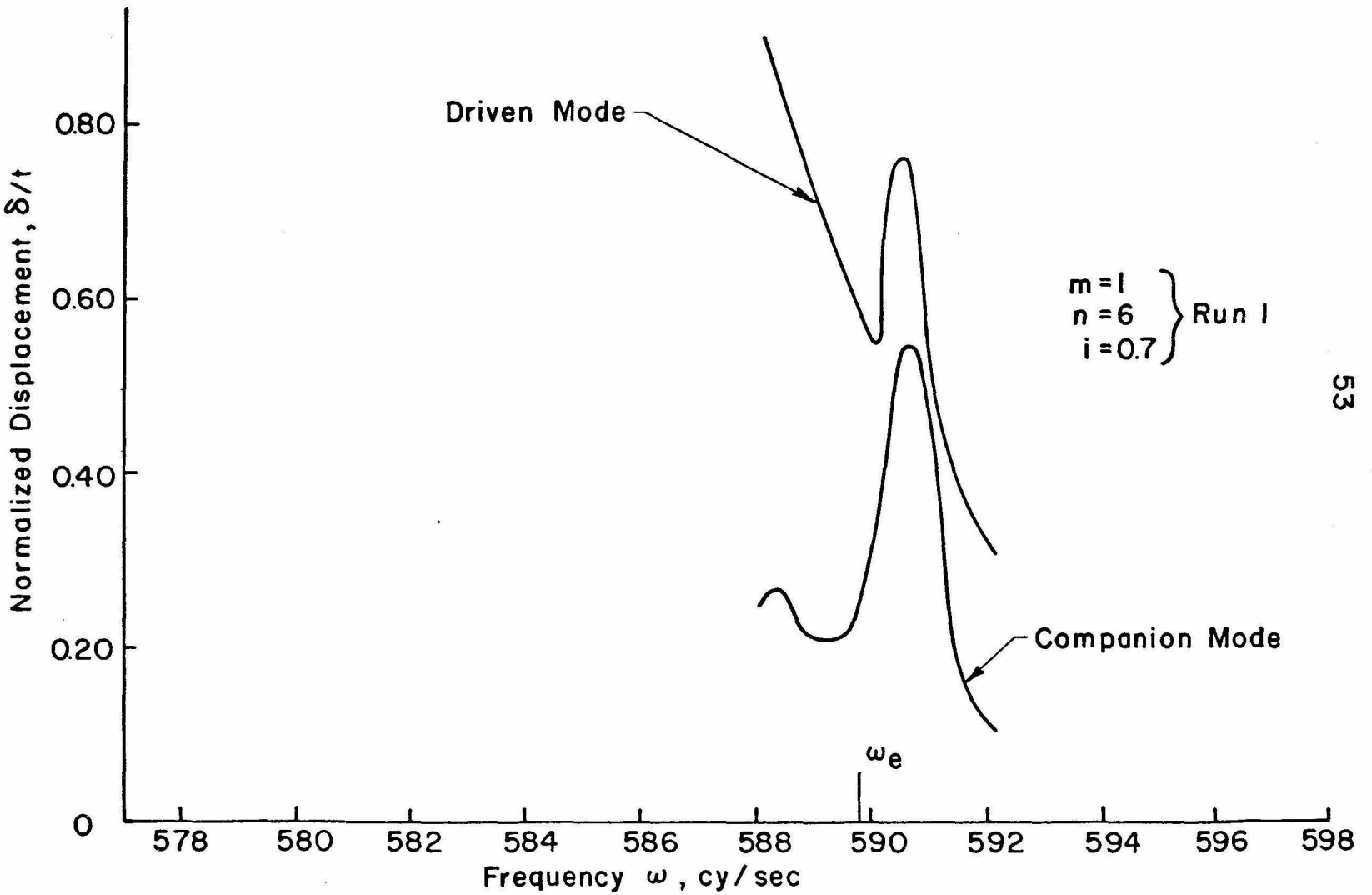

FIG. 19 DRIVEN AND COMPANION MODE RESPONSE, SCANNED DATA

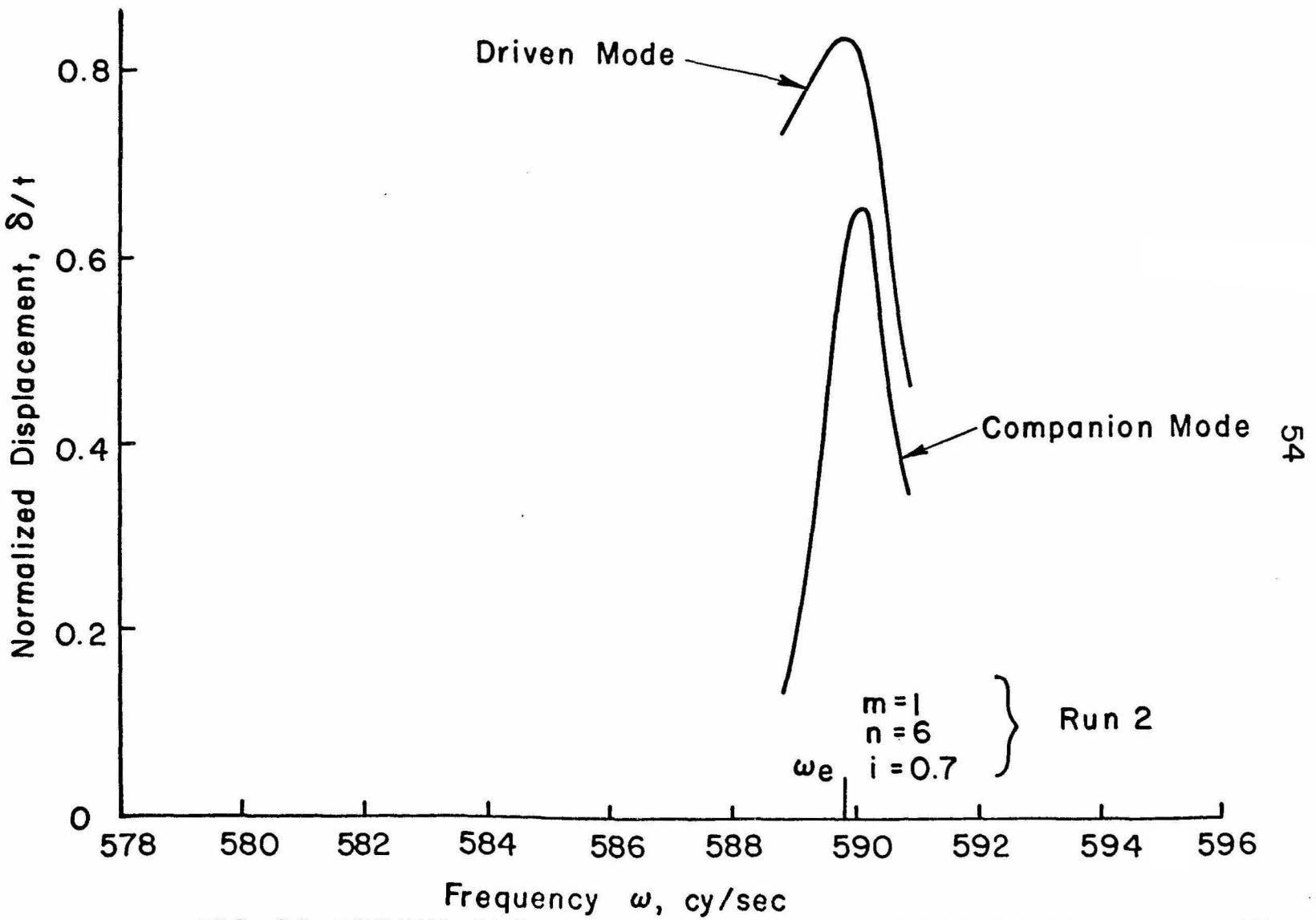

FIG. 20 DRIVEN AND COMPANION MODE RESPONSE, SCANNED DATA

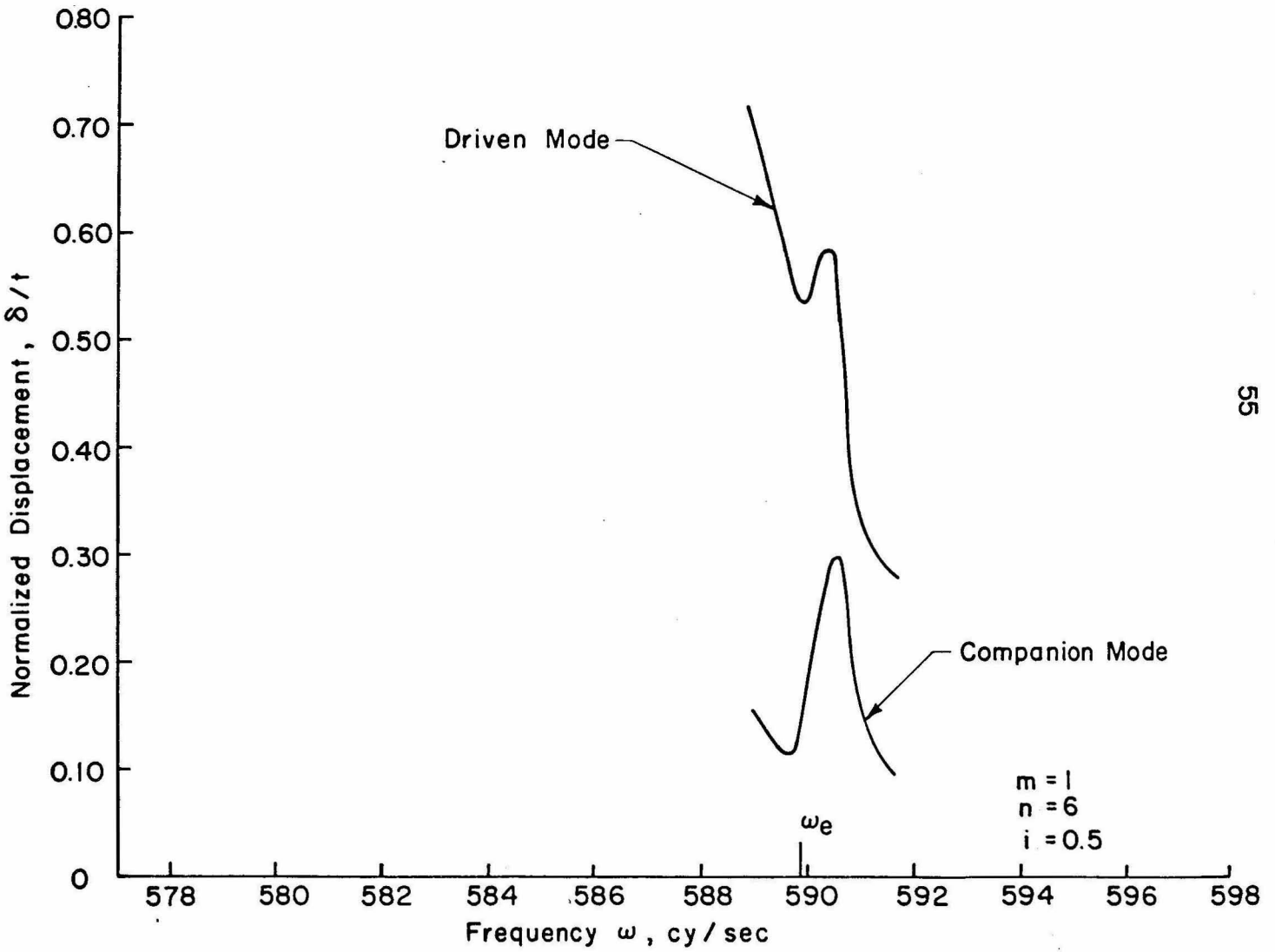

FIG. 21 DRIVEN AND COMPANION MODE RESPONSE, SCANNED DATA

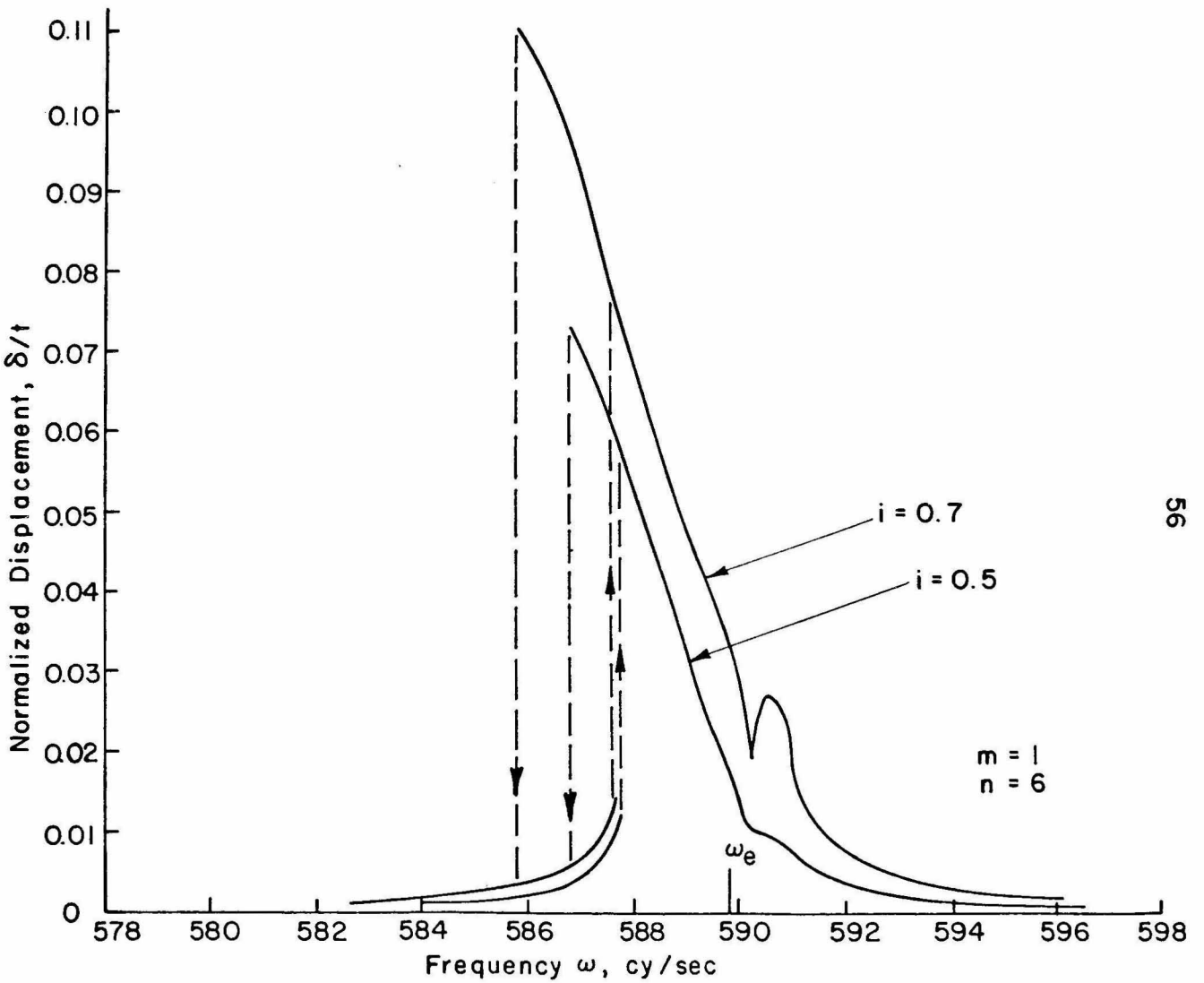

FIG. 22 AXISYMMETRIC MODE RESPONSE

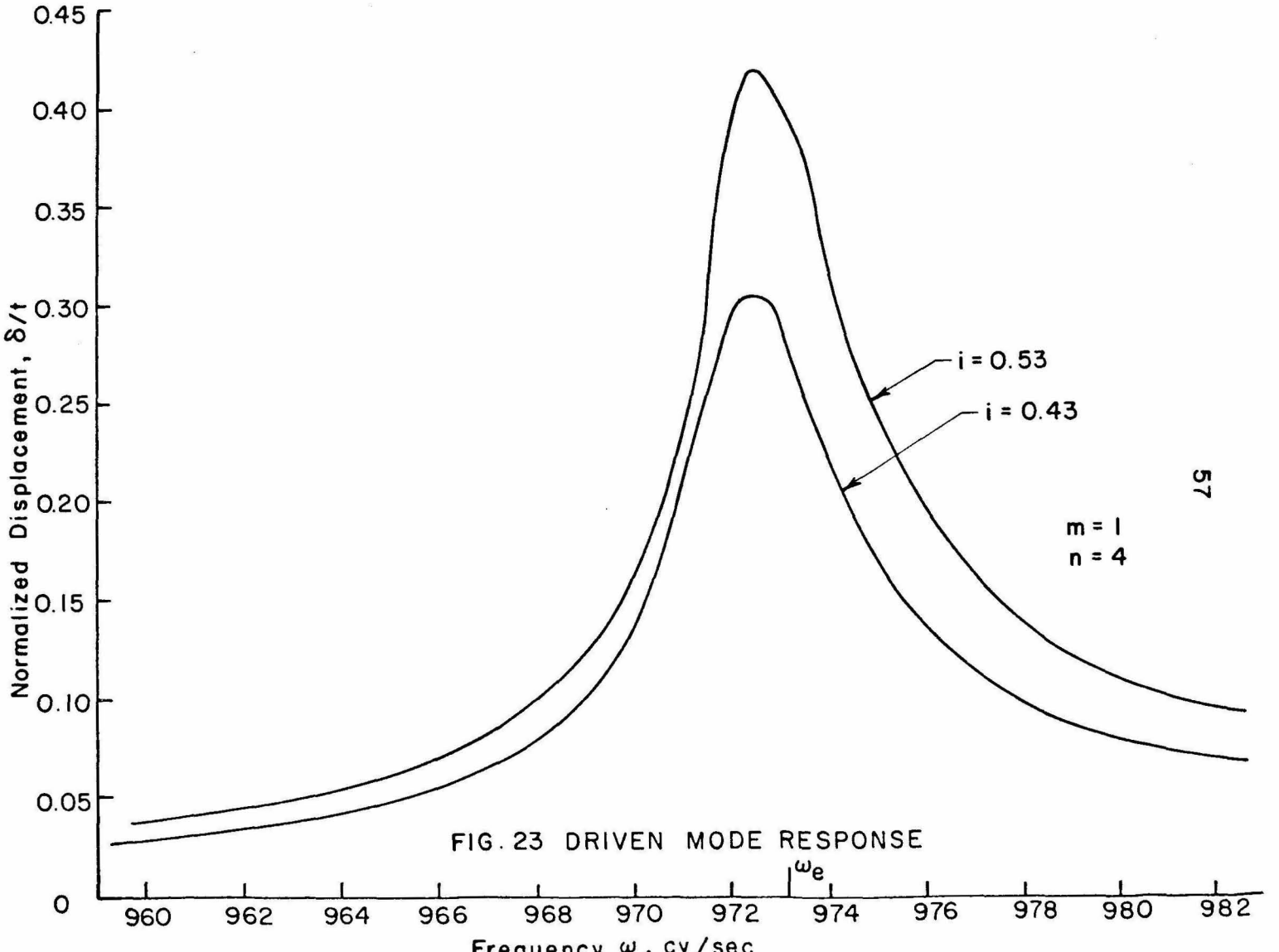

FIG. 23 DRIVEN MODE RESPONSE

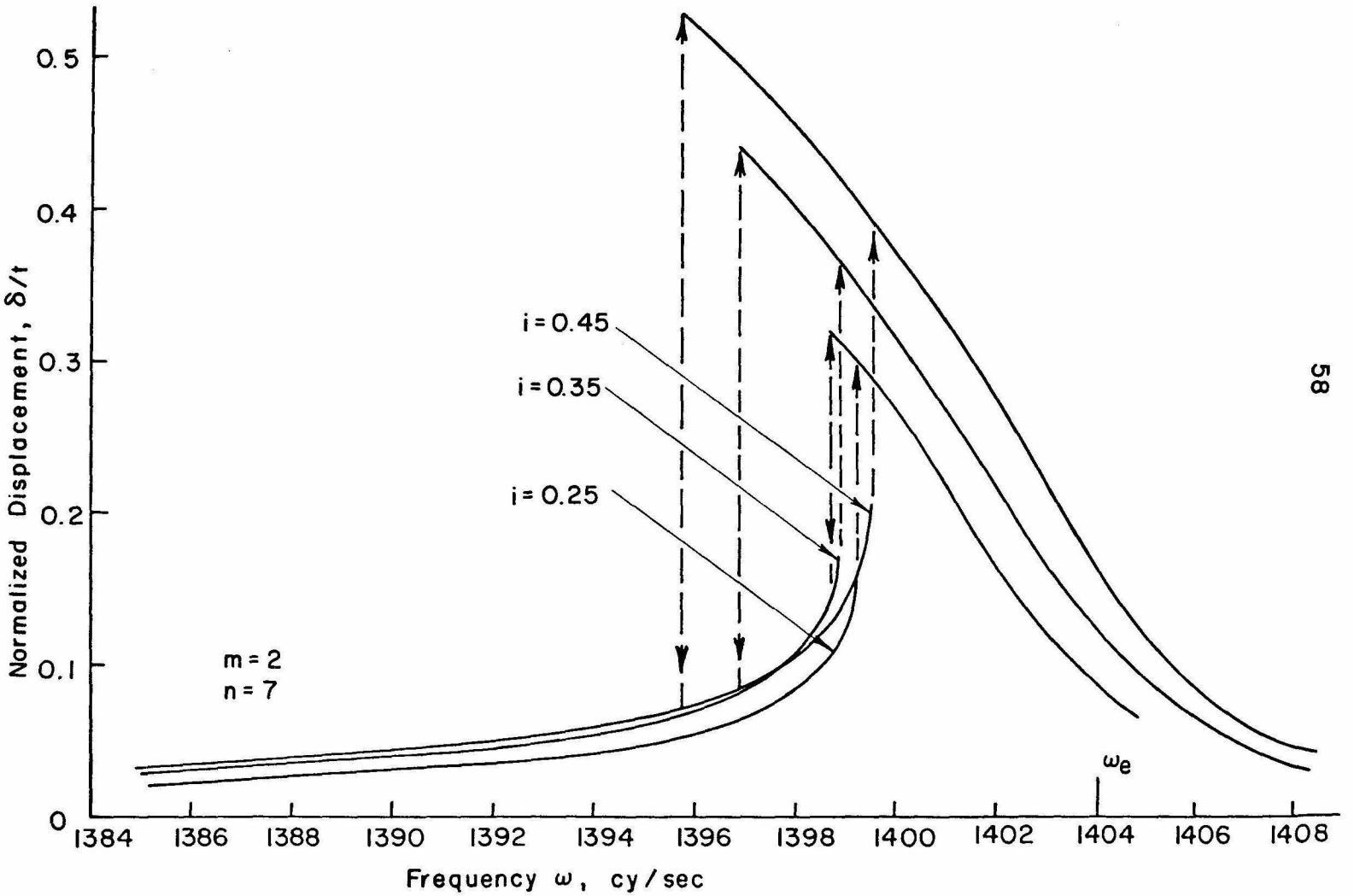

FIG. 24 DRIVEN MODE RESPONSE

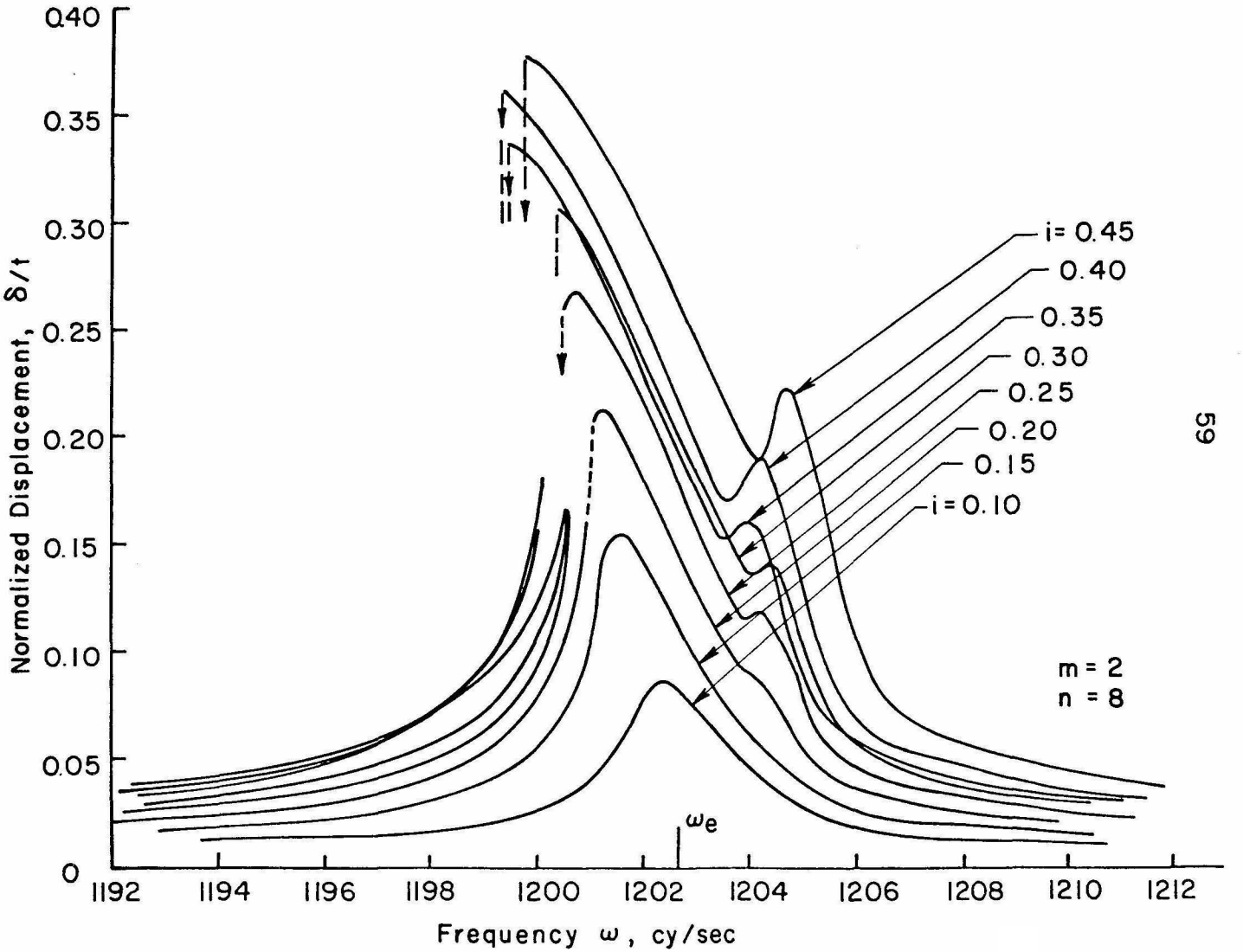

FIG. 25 DRIVEN MODE RESPONSE

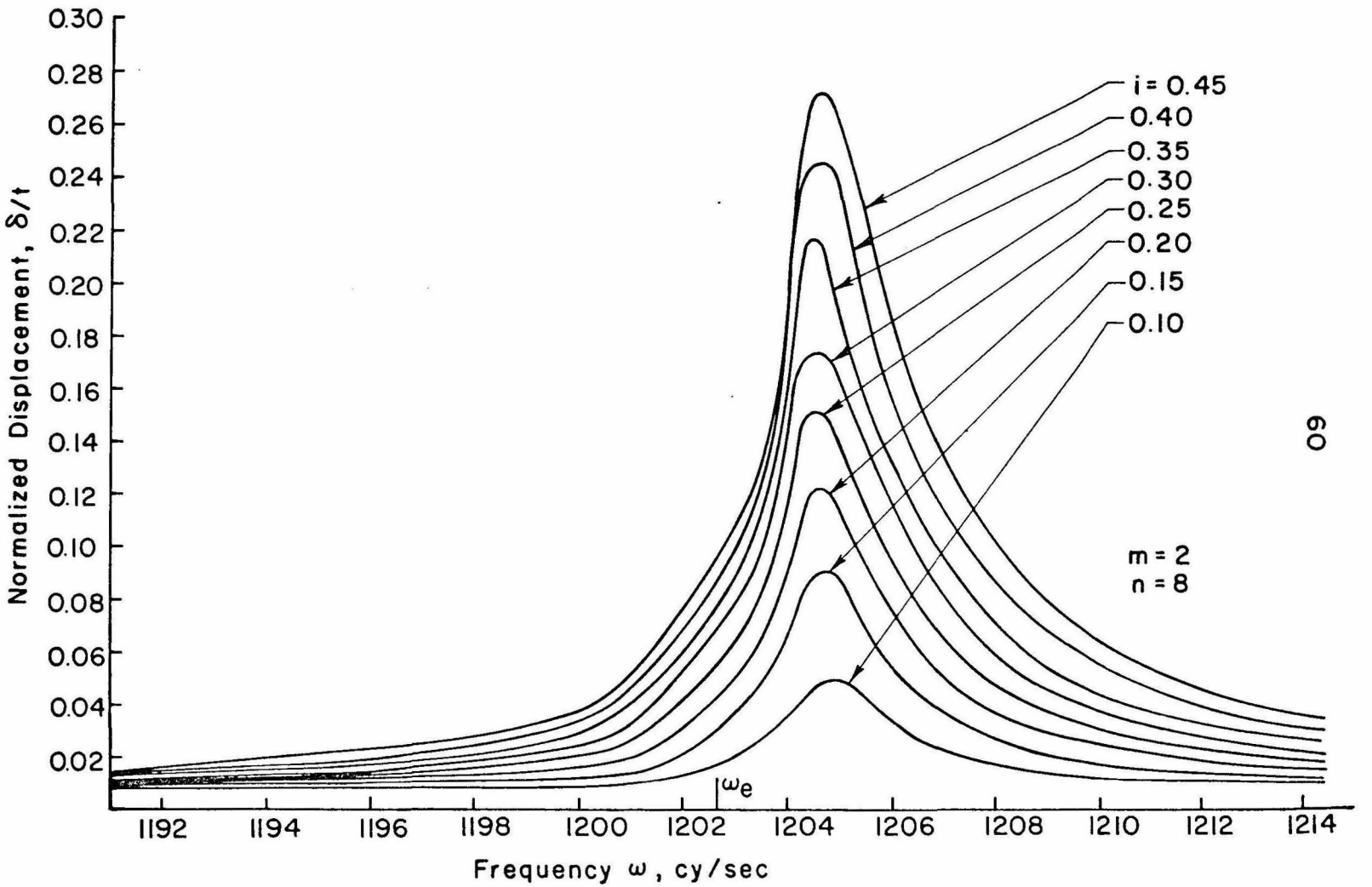

FIG. 26 COMPANION MODE RESPONSE

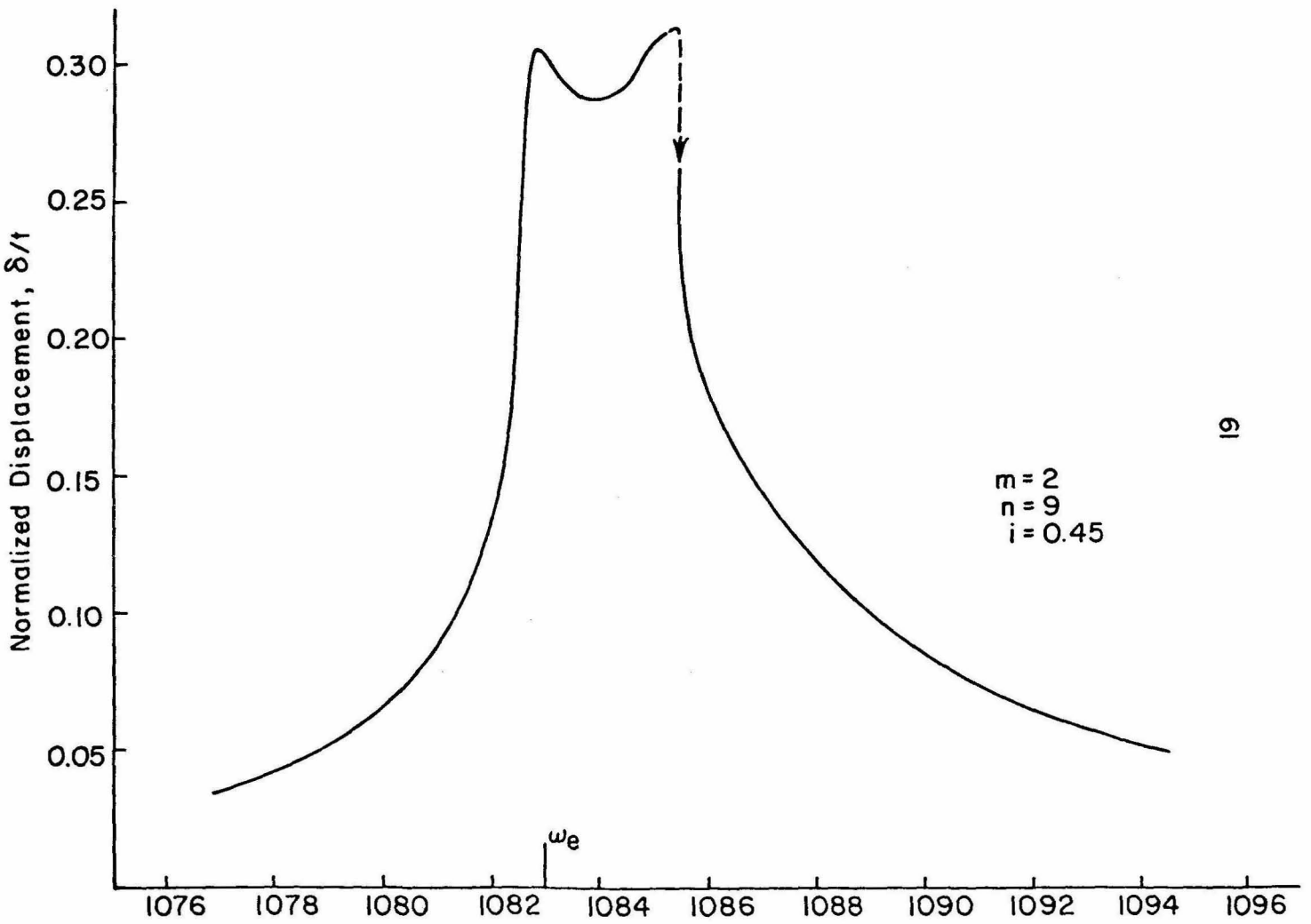

FIG. 27 DRIVEN MODE RESPONSE, STATIONARY DATA

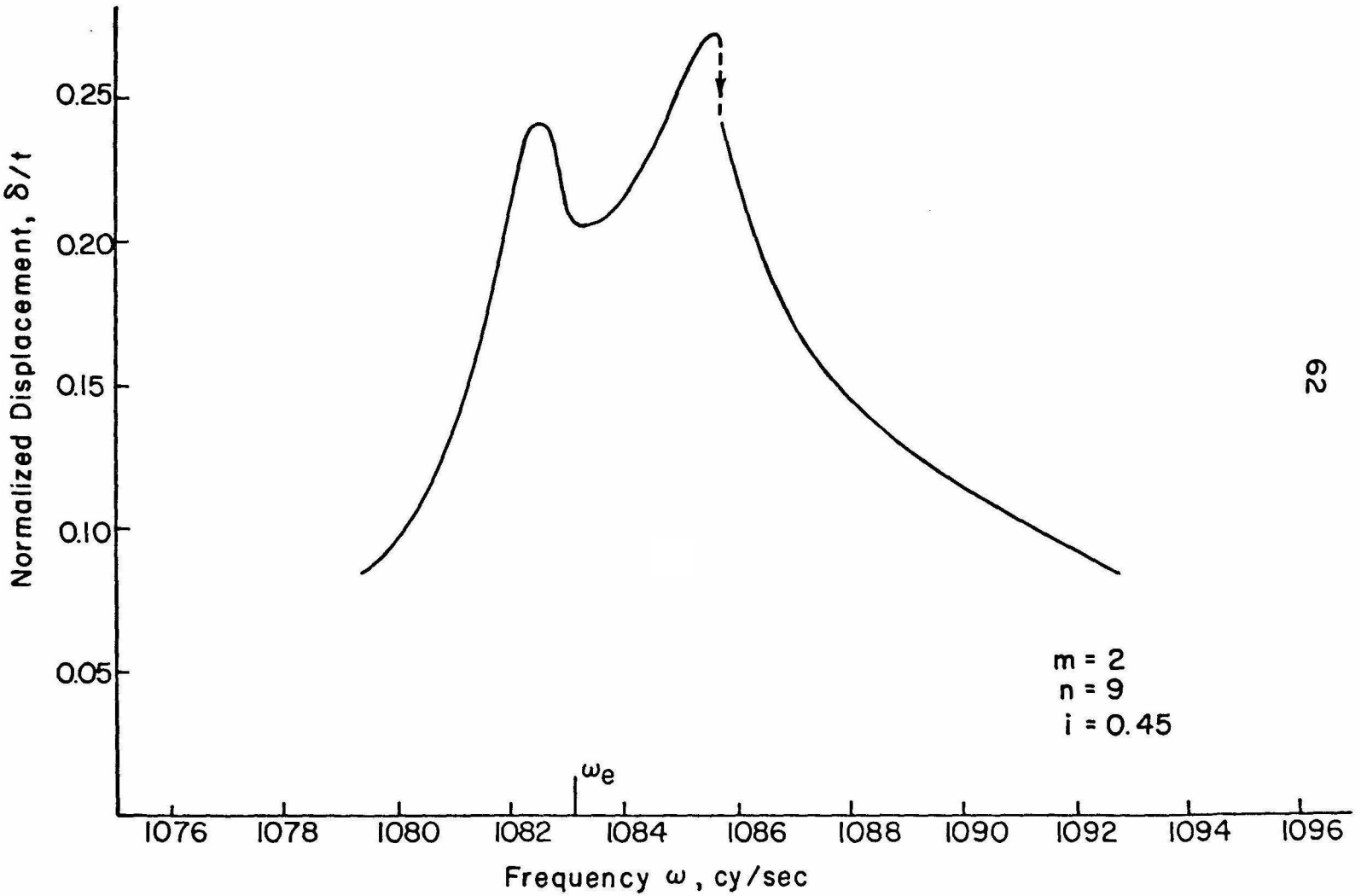

FIG. 28 DRIVEN MODE RESPONSE, SCANNED DATA

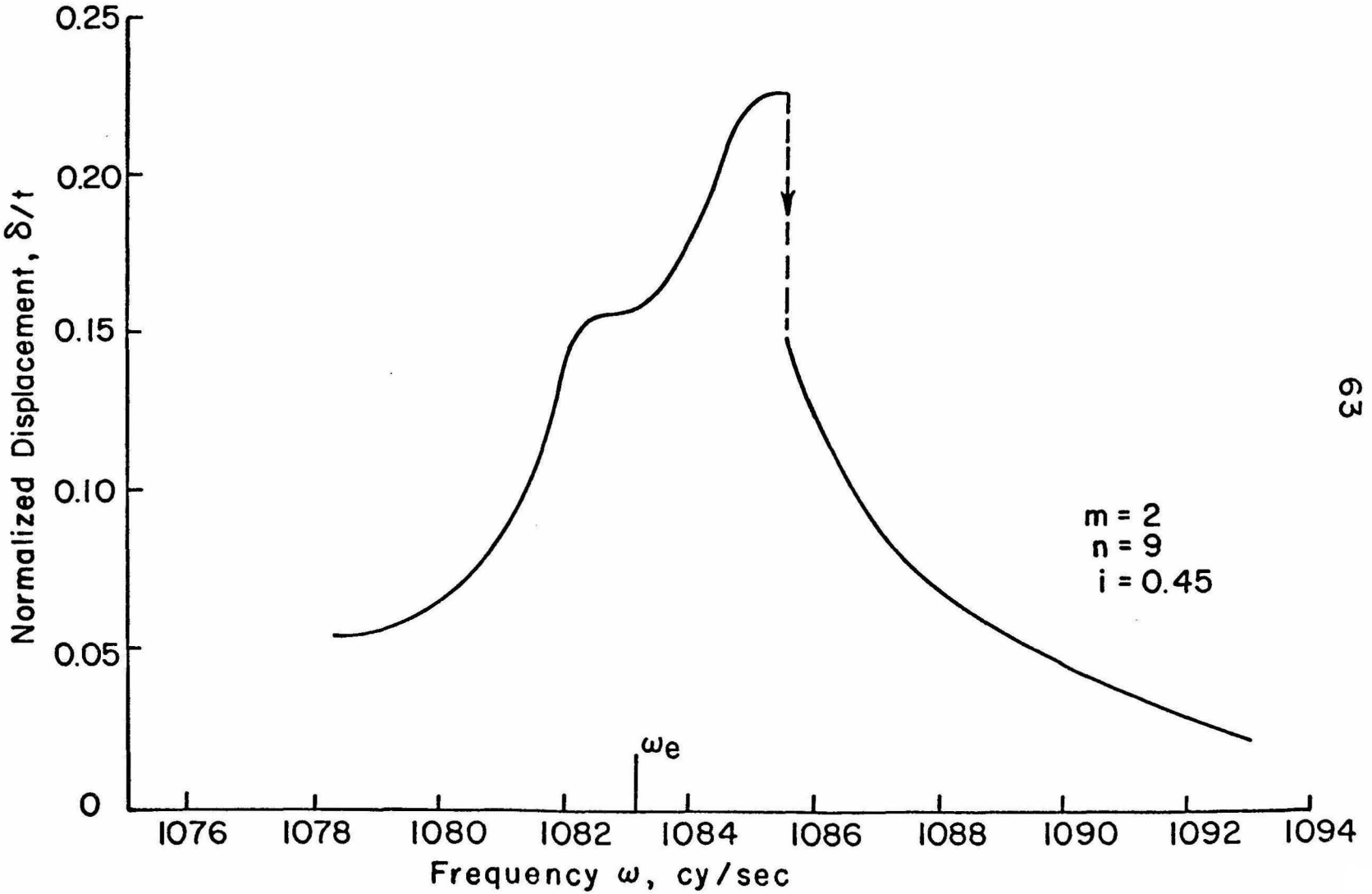

FIG. 29 COMPANION MODE RESPONSE, SCANNED DATA

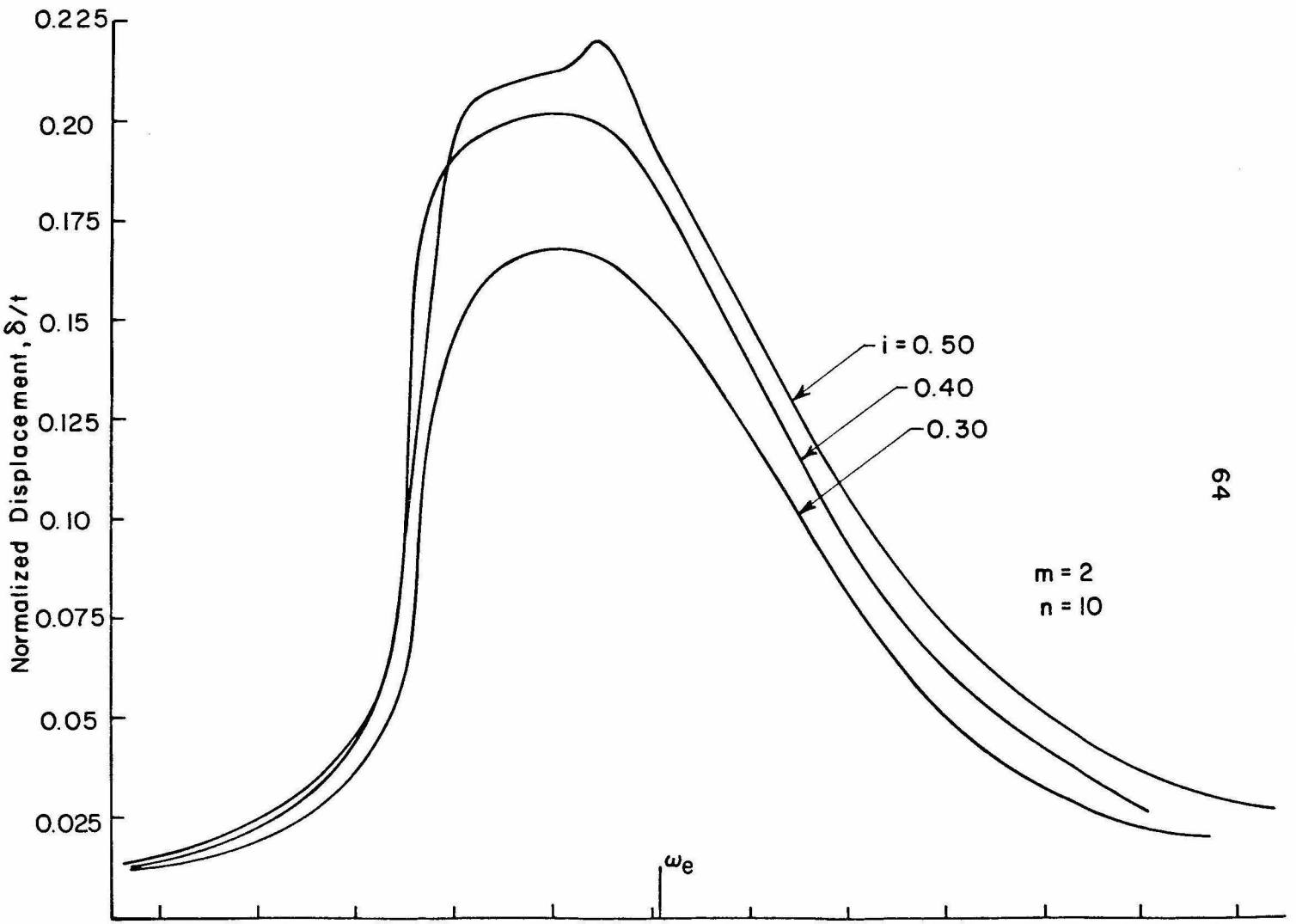

FIG. 30 DRIVEN MODE RESPONSE

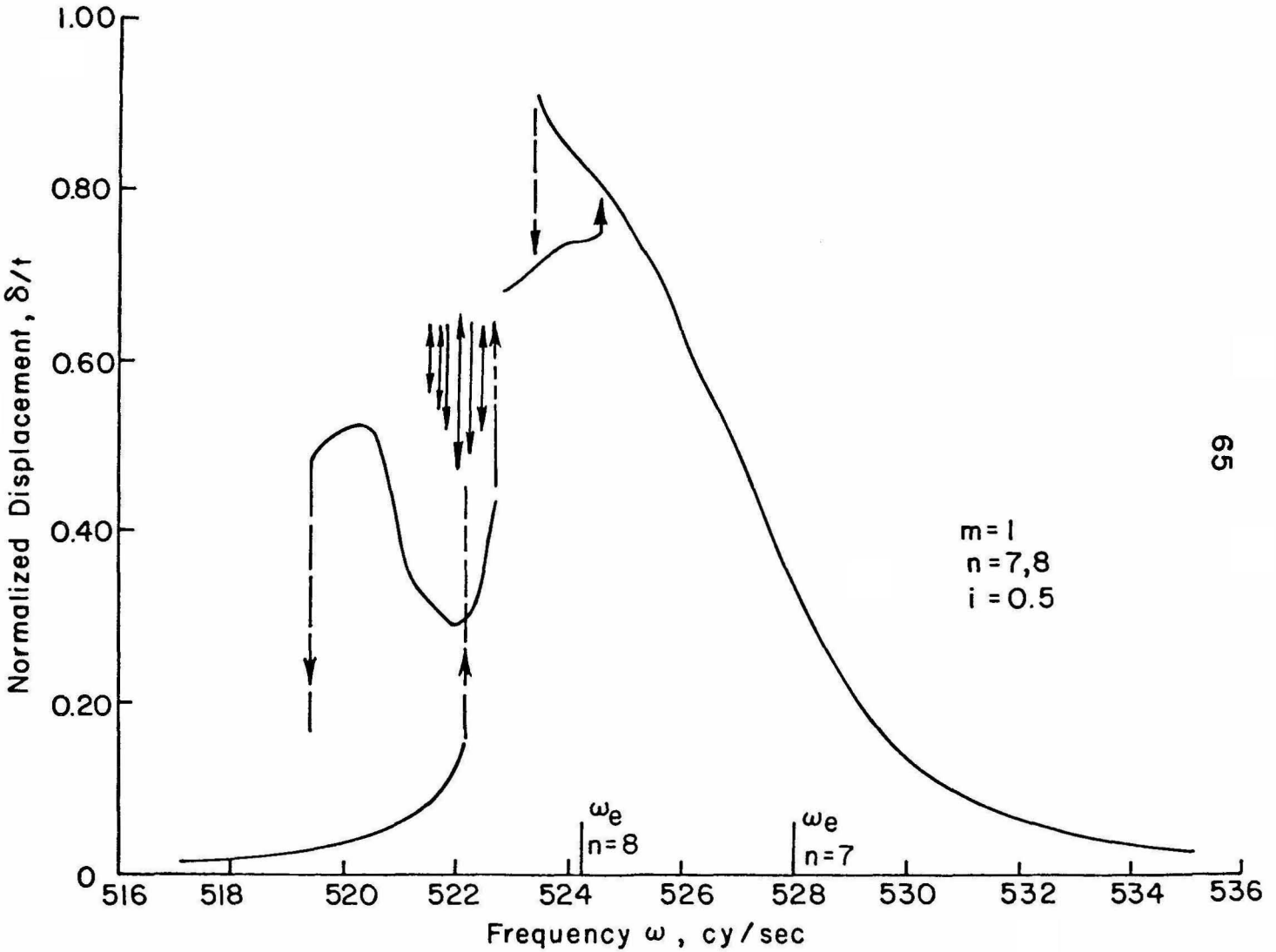

FIG. 31 DRIVEN MODE RESPONSE AND BEAT PHENOMENON